NOAA Technical Report NOS CS 38

NOAA'S GULF OF MAINE OPERATIONAL FORECAST SYSTEM (GOMOFS): MODEL DEVELOPMENT AND HINDCAST SKILL ASSESSMENT

Silver Spring, Maryland
June 2019

noaa National Oceanic and Atmospheric Administration

U.S. DEPARTMENT OF COMMERCE
National Ocean Service
Coast Survey Development Laboratory

Office of Coast Survey
National Ocean Service
National Oceanic and Atmospheric Administration
U.S. Department of Commerce

The Office of Coast Survey (OCS) is the Nation's only official chartmaker. As the oldest United States scientific organization, dating from 1807, this office has a long history. Today it promotes safe navigation by managing the National Oceanic and Atmospheric Administration's (NOAA) nautical chart and oceanographic data collection and information programs.

There are four components of OCS:

The Coast Survey Development Laboratory develops new and efficient techniques to accomplish Coast Survey missions and to produce new and improved products and services for the maritime community and other coastal users.

The Marine Chart Division acquires marine navigational data to construct and maintain nautical charts, Coast Pilots, and related marine products for the United States.

The Hydrographic Surveys Division directs programs for ship and shore-based hydrographic survey units and conducts general hydrographic survey operations.

The Navigational Services Division is the focal point for Coast Survey customer service activities, concentrating predominately on charting issues, fast-response hydrographic surveys, and Coast Pilot updates.

NOAA Technical Report NOS CS 38

NOAA'S GULF OF MAINE OPERATIONAL FORECAST SYSTEM (GOMOFS): MODEL DEVELOPMENT AND HINDCAST SKILL ASSESSMENT

Zizang Yang, Philip Richardson, Yi Chen, Edward P. Myers, and Frank Aikman
Office of Coast Survey, Coast Survey Development Laboratory,
Silver Spring, Maryland

John G.W. Kelley
Office of Coast Survey, Coast Survey Development Laboratory
Durham, New Hampshire

Machuan Peng and Aijun Zhang
Center for Operational Oceanographic Products and Services
Silver Spring, Maryland

June 2019

noaa **National Oceanic and Atmospheric Administratio**

U. S. DEPARTMENT OF COMMERCE **Wilbur Ross,** **Secretary**	**National Oceanic and Atmospheric Administration** **Benjamin Friedman,** **Deputy Under Secretary**	**National Ocean Service** **Nicole R. LeBoeuf,** **Acting Assistant Administrator**

Office of Coast Survey
Rear Admiral Shepard Smith

Coast Survey Development Laboratory
Neeraj Saraf
Acting Division Chief

NOTICE

Mention of a commercial company or product does not constitute an endorsement by NOAA. Use for publicity or advertising purposes of information from this publication concerning proprietary products or the tests of such products is not authorized.

Table of Contents

LIST OF FIGURES

LIST OF TABLES

EXECUTIVE SUMMARY

The National Ocean Service (NOS) of the National Oceanic and Atmospheric Administration (NOAA) has developed an operational nowcast/forecast system for the Gulf of Maine region called the Gulf of Maine Operational Forecast System (GoMOFS). The goal is for the system to produce real-time nowcasts and short-range forecast guidance for water levels, 3-dimensional currents, water temperature, and salinity. This technical report describes the GoMOFS development and the skill assessment of the hindcasts.

GoMOFS uses the Regional Ocean Modeling System (ROMS) as its core hydrodynamic model. The model domain extends from the Rhode Island coast northeastward to the mid-coast of Nova Scotia, Canada, with an open ocean boundary extending beyond the shelf break south of Georges Bank. The model grid has horizontal dimensions of 1173 by 777 with about 700-m resolution and is configured with 30 sigma layers.

The development involved two scenarios of model simulation: a half-year tidal forcing only simulation (Chapter 4) and a one-year (2012) hindcast simulation driven by the full suite of forcing factors (Chapter 5). The hindcast setup used the ROMS wetting and drying feature, a quadratic bottom friction scheme, and the two-equation model of the Mellor-Yamada Level 2.5 turbulence closure scheme. For the open ocean boundary, the implicit Chapman condition for a free surface was adopted, along with the Flather condition for 2-D momentum, and the radiation-nudging condition for 3-D water temperature, salinity, and velocity.

The performance of both the tidal only simulation and the hindcast runs were evaluated using the standard NOS skill assessment software package (Zhang et al, 2006) (Chapters 4 and 5). Model output of water level, currents, temperature, and salinity were evaluated against in-situ observations collected from the NOS Center for Operational Oceanographic Products and Services (CO-OPS) water level and meteorological observation stations, and from buoys of the NWS National Data Buoy Center (NDBC) and the Northeastern Regional Association of Coastal Ocean Observing Systems (NERACOOS).

Over the 24 stations, the averaged absolute model-data differences of the tidal amplitude are 3.8, 1.5, 1.1, and 0.4 cm for M_2, S_2, N_2, and K_1, respectively. The corresponding quantities for tide phase are 2.3, 4.3, 2.5, and 2.6 degrees. Hindcast results also demonstrate favorable model-data agreement. Averaged over observation stations, the root-mean-squared errors and central frequencies are about 0.12 m and 80-90% for water level, less than 1.5 ^{o}C and above 90% for temperature, less than 1 psu and above 90% for salinity, and about 0.15 m/s for current speed and less than 16 degrees for phase. Figure E.1(a)-(f) illustrate the color coded RMSE of water level, temperature, salinity, current speed and phase at each station. The plots reveal the spatial distribution of the error fields. Details of the skill assessment results are presented in Chapters 4 and 5. In general, model skill meets the NOS skill assessment standards.

The GoMOFS development and performance verification have been completed. NOS implemented the hindcast setup in the NOS standard high-performance computer (HPC)-COMF environment. Pre-operational tests were conducted on NOAA Weather and Climate Operational

Supercomputing System (WCOSS) operated by the National Centers for Environmental Predictions (NCEP). GoMOFS began operationally on January 10, 2018.

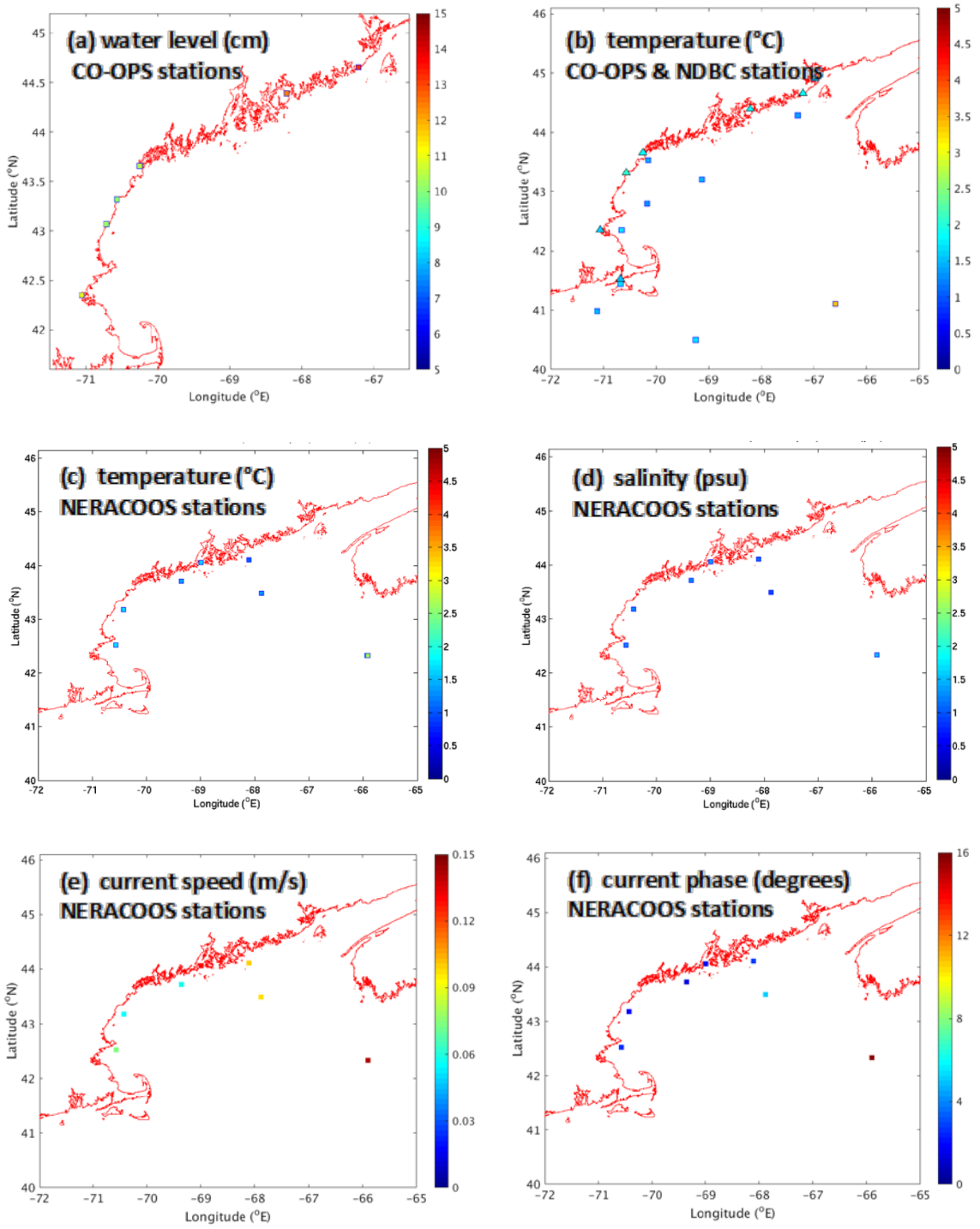

Figure E.1. Color-coded maps of model rmse for (a) water level, (b) water temperature (t) at both co-ops (triangles) and ndbc (squares) stations, (c) t at neracoos buoys, (d) s at neracoos buoys, (e) current speed and (f) current phase at neracoos buoy

1. INTRODUCTION

The Gulf of Maine (GoM) is a semi-enclosed coastal basin located along the coastline of the northeastern U.S. (Figure 1). It is surrounded by the New England coast to the west and to the north. It is adjacent to the Bay of Fundy (BF) to the northeast and it is bounded by the coast of Nova Scotia to the east. To the south, the Gulf water communicates with the open Atlantic Ocean through a series of shoals, banks and channels, such as Nantucket Shoals (NS), the Great South Channel (GSC), Georges Bank (GB), the Northeast Channel (NEC), and Brown Bank (BB).

The GoM/GB system demonstrates a broad variety of physical oceanography phenomena such as a complicated circulation system, intense tidal currents, fronts, internal tides, etc. Baroclinic hydrography, tidal dynamics, and meteorological forcing are the major causal factors. Their relative significance varies spatially, as well as seasonally.

The area is well known for its significant tidal fields. The tidal range is greater than 3 m along the northern and western coast and over 5 m in the BF. The tidal currents are as high as 0.5 to 1 m/s over the NS and GB. The tidal dynamics are heavily involved in the formation of the circulation, fronts, etc. Within the Gulf, tides are forced by ocean tides along the shelf break.

Researchers have explored the hydrodynamics of the area using various types of numerical models including finite difference (Greenberg, 1983; Chen et al., 2001; Xue et al., 2000), finite element (Naimie et al., 1994; Yang and Myers, 2008; Yang et al. 2013), and finite volume (Chen et al., 2011) models. Greenberg (1983) and Naimie et al. (1994) investigated the tidal dynamics of the M_2 astronomical constituent. Using the ADvanced CIRCulation model (ADCIRC) (Westerink et al., 1993), Yang and Myers (2008) investigated the pathway and intensity of the barotropic M_2 tidal energy flux. Chen et al. (2001) studied both barotropic and internal tidal dynamics in the region using the Finite Volume Coastal Ocean Model (FVCOM).

Several of the numerical studies focused on investigating the three-dimensional (3-D) hydrodynamics of the area. Naimie et al. (1994) studied summer season stratification in the GB area using the unstructured-grid finite element model QUODDY. Chen et al. (2001) used a modified Princeton Ocean Model called the Estuarine, Coastal and Ocean Model (semi-implicit) (ECOM-si) to investigate the dynamics of the tidal current rectifications and its impact on the formation of upwelling in the GB region. Xue et al. (2000) simulated the seasonal circulations using the Princeton Ocean Model (POM). Gangopadhyay et al. (2003) developed a multiscale feature model to study the characteristic physical circulation features. To support the Gulf of Maine Ocean Observing System (GoMOOS) operations, Xue et al. (2005) developed a POM-based nowcast/forecast system to produce real-time, 3-D, distribution of circulation and water properties. More recently, Wilkin et al. (2013) developed the data-assimilative "Doppio" real-time and reanalysis ROMS system to make forecasts of hydrodynamics for the broad Mid-Atlantic Bight and the GoM regions.

The National Ocean Service (NOS) of the National Oceanic and Atmospheric Administration (NOAA) has been working on developing an operational oceanographic nowcast/forecast system for the Gulf of Maine (GoMOFS) (Yang et al., 2016). GoMOFS is intended to produce real-time nowcasts and short-range forecast guidance for water levels, 3-dimensional currents, water temperature, and salinity over the broad GoM region. It will support the GoM harmful algal bloom

(HAB) forecast, marine navigation, emergency response, and the environmental management communities.

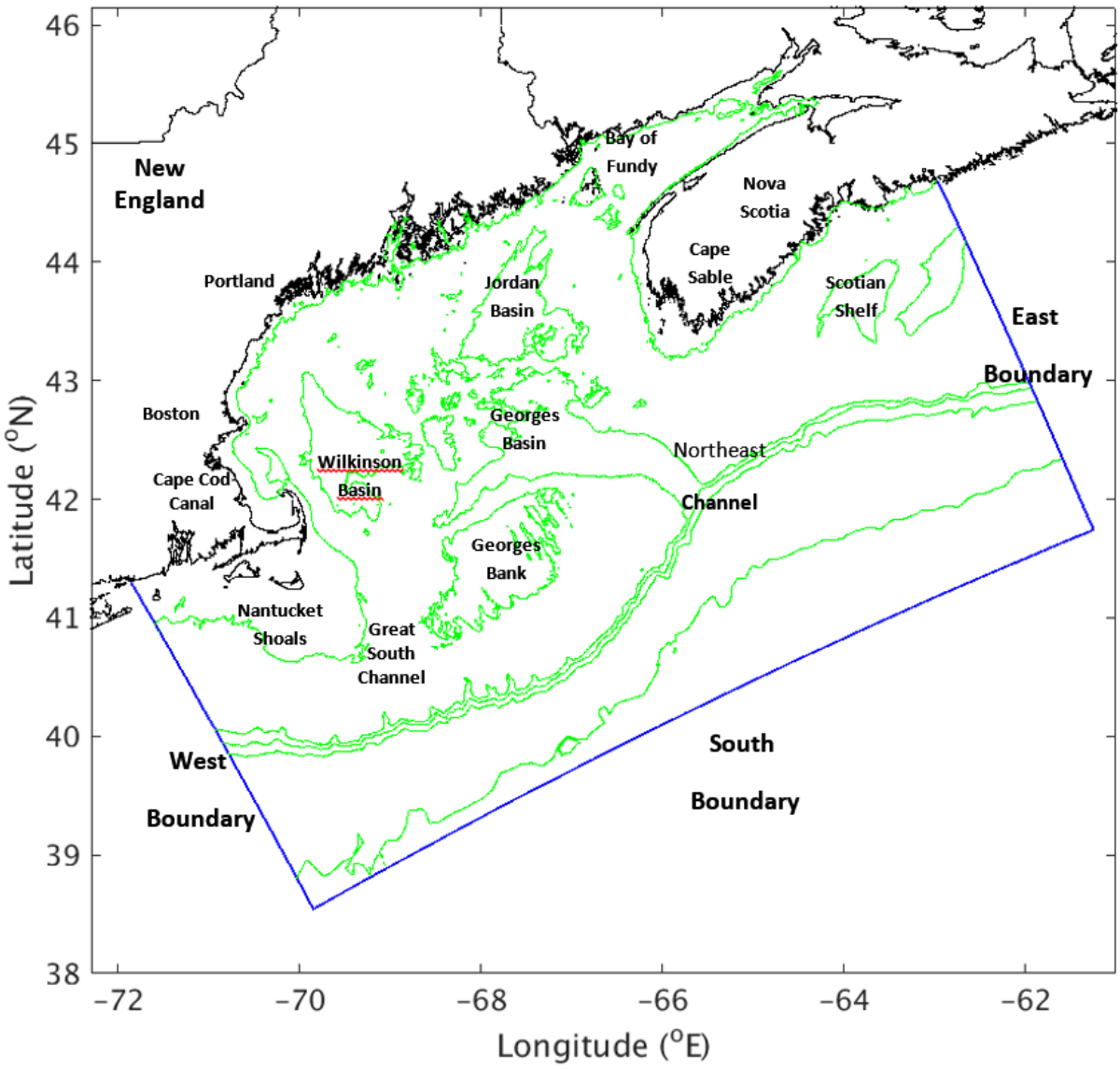

Figure 1. Map of the gulf of maine (gom)/georges bank (gb) region and the gomofs model domain. Green lines represent the 50, 200, 500, 1000, and 3000-m isobaths. Blue lines denote the three open ocean boundaries of the model domain.

GoMOFS adopted the Regional Ocean Model System (ROMS) (Shchepetkin and McWilliams 2003b) as its hydrodynamic model. In developing GoMOFS, we conducted both a six-month constant density tidal simulation and a one-year hindcast simulation for the year of 2012. We evaluated the model performance from both simulations using the NOS standard skill assessment software (Zhang et al., 2006).

This report describes the configuration of the system's hydrodynamic modeling component, the setup of the tidal and hindcast simulations, and the associated skill assessment results. Chapter 2 describes the setup of both the tidal and hindcast simulations. Chapter 3 presents the observational data used for the skill assessment. Chapters 4 and 5 report on the skill assessment results of the tidal and hindcast simulations, respectively. A summary and conclusions are given in Chapter 6.

2. MODEL DEVELOPMENT

The computational core of the Gulf of Maine Operational Forecast System (GoMOFS) was implemented using the Regional Ocean Model System (ROMS) (Shchepetkin and McWilliams, 2005). This chapter describes GoMOFS' model domain, horizontal grid, configuration of the vertical co-ordinate, and population of model grid bathymetry.

2.1. Model Domain and Horizontal Grid

The GoMOFS model has a nearly rectangular domain that extends from the eastern Long Island Sound in the west to the shelf of Nova Scotia in the east and extends to the deep ocean outside of the shelf break (see Figure 1). The domain consists of three open ocean boundaries: the western boundary in the eastern Long Island Sound, the southern boundary outside the shelf break to the southeast of the GoM, and the eastern boundary across the shelf of Nova Scotia.

The model consists of an orthogonal grid (Figure 2) with horizontal dimensions of 1177 by 776 (rho-grid) and nearly uniform spatial resolution of approximately 0.7 km. The grid resolves major coastal embayments including Cape Cod Bay, Boston Harbor, Casco Bay, Penobscot Bay, and the Bay of Fundy. Note that the 0.7m resolution is insufficient for the grid to resolve small scale coastal features such as navigation channels and river courses, e.g., the Cape Cod Canal. However, the 0.7-km resolution proves to be sufficient to resolve broad- and medium-scale hydrodynamics within the GoM.

2.2. Configuration of Vertical Coordinates

ROMS has a generalized vertical, terrain-following, S-coordinate system. This system makes available two types of vertical transformation equations, each of which supports numerous vertical stretching functions. Configuration of the vertical coordinate system is specified through five numerical parameters: Vtransform types, Vstretching, THETA_S (θ_s), THETA_B (θ_b), and TCLINE in the ROMS standard main input file. Vtransform and Vstretching represent the type of transformation equation and vertical stretching function, respectively. THETA_S and THETA_B are the surface and bottom stretching parameters, respectively. TCLINE specifies width (in units of meters) of the surface or bottom boundary layer in which higher vertical resolution is needed during stretching.

The GoMOFS model grid is configured with 30 unevenly distributed sigma layers. The five parameters are specified as Vtransform=2, Vstretching=4, THETA_S = 5, THETA_B = 0.4, and TCLINE = 50. The first two parameters represent ROMS default values. THETA_S and THETA_B result in more densely distributed sigma layers near the surface than in the remaining deeper water. TCLINE equal to 50 m was intended to represent roughly the seasonally averaged mixed layer depth throughout the GoMOFS domain.

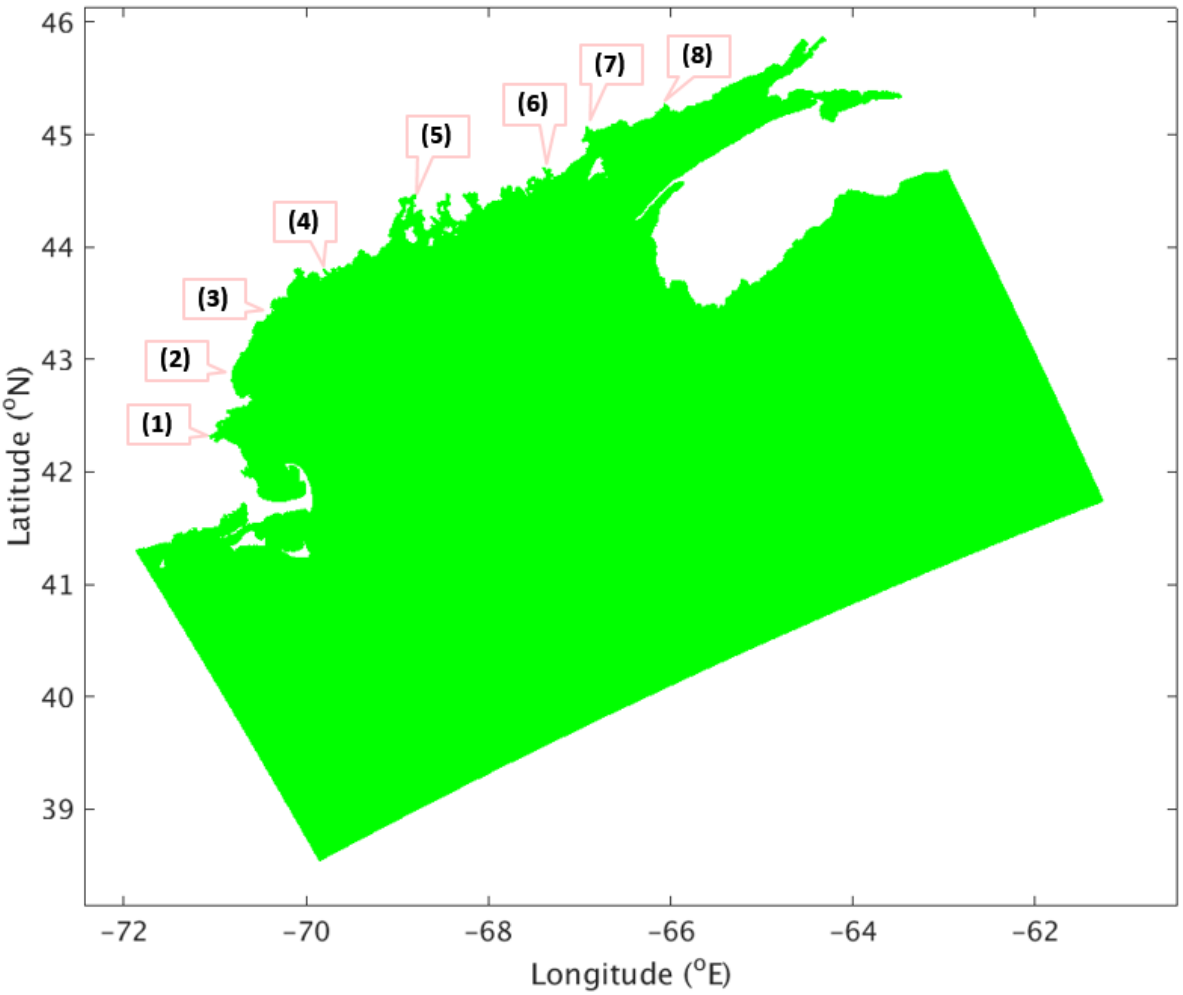

Figure 2. The GoMOFS model grid along with the locations of eight river entrances including (1) Neponset River, (2) Merrimack River, (3) Saco River, (4) Androscoggin and Kennebec Rivers, (5) Penobscot River, (6) Machias River, (7) St. Croix River, and (8) St. Johns River.

2.3. Bathymetry

The bathymetry of the model grid was calculated by a linear interpolation of the combined VDatum ADCIRC model grid bathymetry (Yang et al., 2013) and the bathymetry in the 2-minute Gridded Global Relief Data (ETOPO2) (National Geophysical Data Center, 2006).

Figure 3 displays a color-filled contour bathymetry map. The model grid resolves key bathymetric features such as Georges Bank, the Northeast Channel, the Great South Channel, etc. The bathymetry ranges from about 3 m in Nantucket Shoals to around 4,324 m along the domain's southeastern boundary.

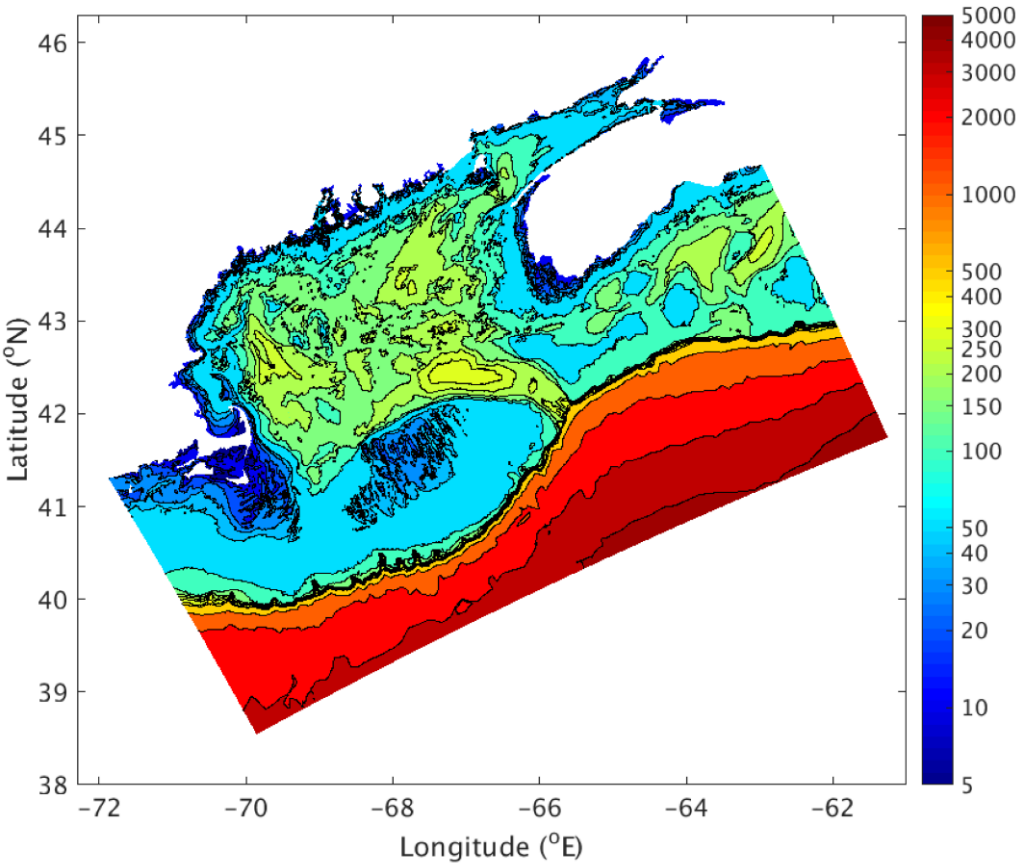

Figure 3. Bathymetry of the model grid. The color bar unit is meter.

2.4. Model Setup and Computation

In developing GoMOFS, two scenarios of model simulations were performed for the year 2012: a tidal forcing only simulation and a hindcast simulation. The model configuration in both simulations remained the same except that the former was initialized with constant water temperature and salinity, and was forced with tidal water level and currents on the open ocean boundary. The latter was driven with the total water level and currents that include both tidal and sub-tidal components on the open ocean boundary, sea-surface meteorological forcing, and river forcing. The purpose of conducting the tidal only simulation was to optimize the configuration of the tidal open ocean boundary forcing to ensure a favorable model performance in reproducing realistic water levels.

GoMOFS uses the ROMS wetting and drying feature, a quadratic bottom friction scheme, as well as the two-equation model of the “revised” Mellor-Yamada Level 2.5 turbulence closure scheme (GLS/k-kl) implemented through the ROMS generic length scale (GLS) module (Warner et al, 2005).

For the open ocean boundary, we adopted the implicit Chapman condition for the free surface, the Flather condition for the 2-D momentum, and the radiation-nudging condition for the 3-D temperature, salinity, and velocity.

The hindcast simulation was driven with the complete suite of ambient forcings. These forcings include the open ocean boundary forcing of the combined tidal and subtidal water levels, the 2-dimensional depth-averaged tidal currents, the 3-dimensional temperature (T), salinity (S), and subtidal currents, the river flow at river entrances (Figure 2), and the meteorological forcing on the sea-surface.

For the non-tidal open ocean conditions, GoMOFS used the nowcast results from the NWS Global Real-Time Ocean Forecast System (G-RTOFS) (Mehra and Rajan, 2015). G-RTOFS is operated by the NOAA National Centers for Environmental Prediction (NCEP). G-RTOFS is based on the Naval Oceanographic Office's configuration of the 1/12° eddy resolving Global Hybrid Coordinates Ocean Model (HYCOM). This ocean model has horizontal dimensions of 4500 by 3298 and has 32 vertical hybrid layers (isopycnals in the deep water, isolevels in the mixed layer, and sigma in shallow waters). The system assimilates in-situ profiles of temperature and salinity from a variety of sources as well as remotely sensed SST retrievals, SSH, and sea-ice concentrations. G-RTOFS is forced with 3-hourly momentum, radiation, and precipitation fluxes from the operational NCEP Global Forecast System (GFS). GFS produced nowcast and forecast guidance of SSH, SST, and SSS at three hourly intervals, and full volume parameters (3-dimensional temperature, salinity, currents, and mixed layer depths) at six hourly intervals. The nowcast outputs of the three-hourly water level and the six-hourly 3-D currents and T/S as the non-tidal forcing were spatially interpolated onto the GoMOFS model grid's open ocean boundaries and temporally interpolated across the entire 2012 hindcast period.

The river forcing includes discharge from nine rivers along the Gulf coast. These include from north to south: the St. John River, St. Croix River, Machias River, Penobscot River, Kennebec River, Androscoggin River, Saco River, Merrimack River, and the Neponset River. Figure 2 illustrates their entrances on the model grid. Note that the Androscoggin and Kennebec Rivers merge downstream near the coast.

The river discharge and water temperature data are from U.S. Geological Survey (USGS) river discharge observations (data available at https://waterdata.usgs.gov/nwis). Note that the locations of the river discharge observations are usually far inland from the river mouth. In the hindcast setup, the magnitude of the discharge was increased by 20% to foster a favorable model-data agreement of salinity. This factor was determined empiriaclly through a series of trial-and-error model run experiments.

The salinity was specified to be zero for all nine rivers. The assumption of zero salinity is the recourse that was decided upon after considering data availability, the model grid configuration for the river course, and the skill of the hindcast run results. The GoMOFS model grid extends into each river by a distance of four to ten kilometers rather than defining the river entrance by the nodes immediately along the open coast. The distances from the open coast might not be deep enough to fully justify the zero salinity assumption. However, there was a lack of salinity observations of the river discharge. Hence, the informal common practice was applied which

involves specifying zero salinity value rather than choosing some other arbitrary value. As an ad hoc justification for the zero-salinity assumption and for the adjusted discharge, the hindcast salinity demonstrated reasonably good agreement with the observations.

The hindcast made use of the 12-km resolution forecast guidance of the NWS National Centers for Environmental Predictions (NCEP's) North American Mesoscale (NAM) forecast modeling system for surface forcing. The ROMS model used the 10-m wind velocity to compute the surface wind stress, 2-m surface air temperature and relative humidity, total shortwave radiation, and downward longwave radiation. The ROMS used the bulk flux formulation to calculate the air-sea momentum and heat fluxes; it used the evaporation and precipitation rates to calculate the net salinity flux across the air-sea interface.

The hindcast simulation ran from 1 January to 31 December 2012. It started from a still water state with the T/S fields initialized with G-RTOFS nowcasts. Following an initial 5-day ramping up, the model run continued for another 10 days to ensure that an equilibrium state was reached. The time series of the ocean state variables (water level, currents, and T/S) were recorded at 6 minute intervals from the 15th day to the end of the hindcast run. These time series were used to evaluate the model performance using the NOS standard skill assessment software (Zhang et al., 2006).

3. OBSERVATIONAL DATA

Observational data are used to verify the hindcast results and to assess the GoMOFS skill level. The data include harmonic constants of tidal water levels and observed time series data of water level, temperature, and salinity in the hindcast period (2012).

3.1. Tidal Harmonic Constants

Tidal harmonic constants were acquired from the archives of the NOS CO-OPS. The harmonic constants were derived from water level measurements at National Water Level Observation Network (NWLON) stations maintained by CO-OPS. The online site of the data source is https://tidesandcurrents.noaa.gov/stations.html?type=Harmonic+Constituents. Data from a total of 24 stations were used to verify the results of the constant density tidal simulations (Section 1). Table 1 lists the station names, identification numbers (IDs), and digital geographic locations in longitude and latitude.

Table 1. NOS Station IDs, names, and geographic locations of tidal harmonic constant stations

No	Station ID	Station Name	Longitude	Latitude
1	8411250	Cutler Naval Base, ME	-67.297	44.642
2	8411060	Cutler Farris Wharf, ME	-67.21	44.657
3	8412581	Milbridge, ME	-67.875	44.54
4	8413320	Bar Harbor, ME	-68.205	44.392
5	8413825	Mackerel Cove, ME	-68.435	44.17
6	8414249	Oceanville, Deer Isle, ME	-68.62	44.192
7	8414721	Fort Pt., ME	-68.813	44.472
8	8414888	Penobscot Bay, ME	-68.887	44.157
9	8417177	Hunniwell, ME	-69.785	43.755
10	8418150	Portland, ME	-70.247	43.657
11	8418445	Pine Point, ME	-70.333	43.545
12	8418606	Saco River, ME	-70.382	43.462
13	8423898	Fort Point, NH	-70.712	43.072
14	8441551	Rockport Harbor, MA	-70.615	42.658
15	8442645	Salem Harbor, MA	-70.877	42.523

No	Station ID	Station Name	Longitude	Latitude
16	8443187	Lynn Harbor, MA	-70.943	42.458
17	8444162	Boston Light, MA	-70.892	42.328
18	8445138	Scituate Harbor, MA	-70.727	42.202
19	8444525	Nut Island, MA	-70.953	42.28
20	8446009	Green Harbor River, MA	-70.647	42.083
21	8446121	Provincetown, MA	-70.182	42.048
22	8446166	Duxbury Harbor, MA	-70.67	42.038
23	8446493	Plymouth Harbor, MA	-70.662	41.96
24	8447241	Sesuit Harbor, MA	-70.155	41.752

3.2. Water Level

Water level time series data from 2012 from six CO-OPS NWLON stations (Table 2) were used to evaluate the water level performance of the GoMOFS hindcast simulations. Figure 4 shows the station map. Note that some other stations located in the small estuaries, embayments, or inter-island channels which were not resolved by the model grid, were excluded. These include stations 8449130 (Nantucket Island, MA), 8447930 (Woods Hole, MA), 8447435 (Chatham, MA), and 8410140 (Eastport, ME).

The 6-minute interval time series was retrieved from https://tidesandcurrents.noaa.gov/gmap3. To evaluate the model performance of the subtidal water level results, we low-pass filtered the 6-minute data using a Fourier transform filter with a 33-day cutoff frequency to eliminate both the tidal and other high frequency components.

Table 2. Geographic information for CO-OPS water level (WL) and weather stations

No	Station ID	Station Name	Lon (^{o}N)	Lat (^{o}E)	Properties	Temperature Measurement Depths (m)
1	8411060	Cutler Farris Wharf, ME	-67.21	44.657	WL, T	2.4
2	8413320	Bar Harbor, ME	-68.205	44.392	WL, T	2.9
3	8418150	Portland, ME	-70.247	43.657	WL, T	4.9
4	8419317	Wells, ME	-70.563	43.32	WL, T	3.3
5	8423898	Fort Pt., NH	-70.712	43.072	WL	n/a
6	8443970	Boston, MA	-71.053	42.353	WL, T	2.9
7	8447930	Woods Hole, MA	-70.672	41.523	T	2.0
8	8410140	East Port, ME	-66.982	44.903	T	3.3

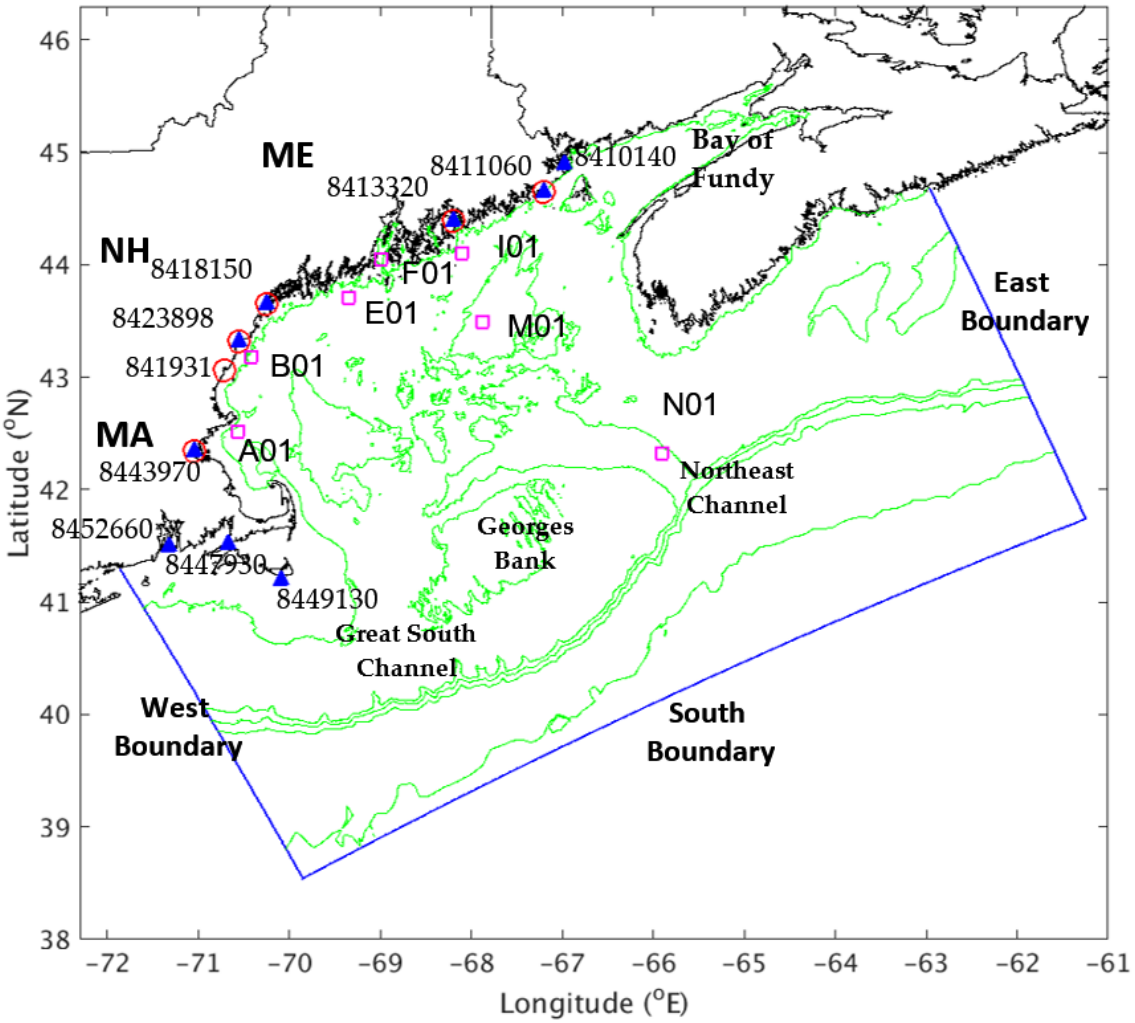

Figure 4. Map of the GOM/GB region and the GoMOFS model domain. Green lines represent the 50, 200, 500, 1000, and 3000-m isobaths. Blue lines denote the three open ocean boundaries of the model domain. Observation stations are the CO-OPS water level stations (re ed circles), CO-OPS water temperature stations (filled blue triangles), and the NERACOOS buoys (magenta squares). The station IDs are labeled near the location markers.

3.3. Temperature, Salinity, and Current Velocity

The water temperature data were obtained from seven CO-OPS weather stations (Table 2), nine NDBC buoys (Table 3), and seven NERACOOS buoys (Table 3.4). All three data sets were downloaded from the NDBC online archive at http://www.ndbc.noaa.gov/data/historical/ocean. The CO-OPS and NDBC data were near surface measurements, whereas the NERACOOS data included both near surface and at-depth measurements. Tables 3 and 4 list the station IDs, names, geographic locations in longitude and latitude, and measurement depths of the CO-OPS, NDBC, and NERACOOS stations, respectively. Figure 5 shows a map of NDBC buoy stations, and Table 5 lists the depths of the NERACOOS buoy measurements.

Table 3. Geographic information on NOS NDBC buoys

No.	Station ID	Lon (^{o}E)	Lat (^{o}N)	Buoy Name	Depths of measurements (m)
1	44005	-69.128	43.204	Gulf of Maine	1.0
2	44007	-70.144	43.531	12 NM SE of Portland, MA	0.6
3	44008	-69.247	40.502	Nantucket	0.6
4	44011	-66.6	41.105	Georges Bank	1.0
5	44013	-70.651	42.346	Boston, MA	0.6
6	44020	-70.672	41.443	Nantucket Main Channel Lighted Buoy, MA	0.6
7	44027	-67.307	44.287	Jonesport ME	0.6
8	44097	-71.117	40.981	Block Island, RI	1
9	44098	-70.168	42.798	Jeffrey's Ledge, NH	0.6

Table 4. Geographic information on NERACOOS buoys

No.	Station ID	Buoy Name	Lon (^{o}E)	Lat (^{o}N)	Location
1	44029	A01	-70.566	42.522	Mass. Bay/Stellwagen, MA
2	44030	B01	-70.428	43.181	Western Maine Shelf, ME
3	44032	E01	-69.358	43.715	Central Maine Shelf, ME

4	44033	F01	-68.997	44.056	West Penobscot Bay, ME
5	44034	I01	-68.109	44.106	Eastern Maine Shelf, ME
6	44037	M01	-67.880	43.491	Jordan Basin, ME
7	44024	N01	-65.907	42.331	Northeast Channel, ME

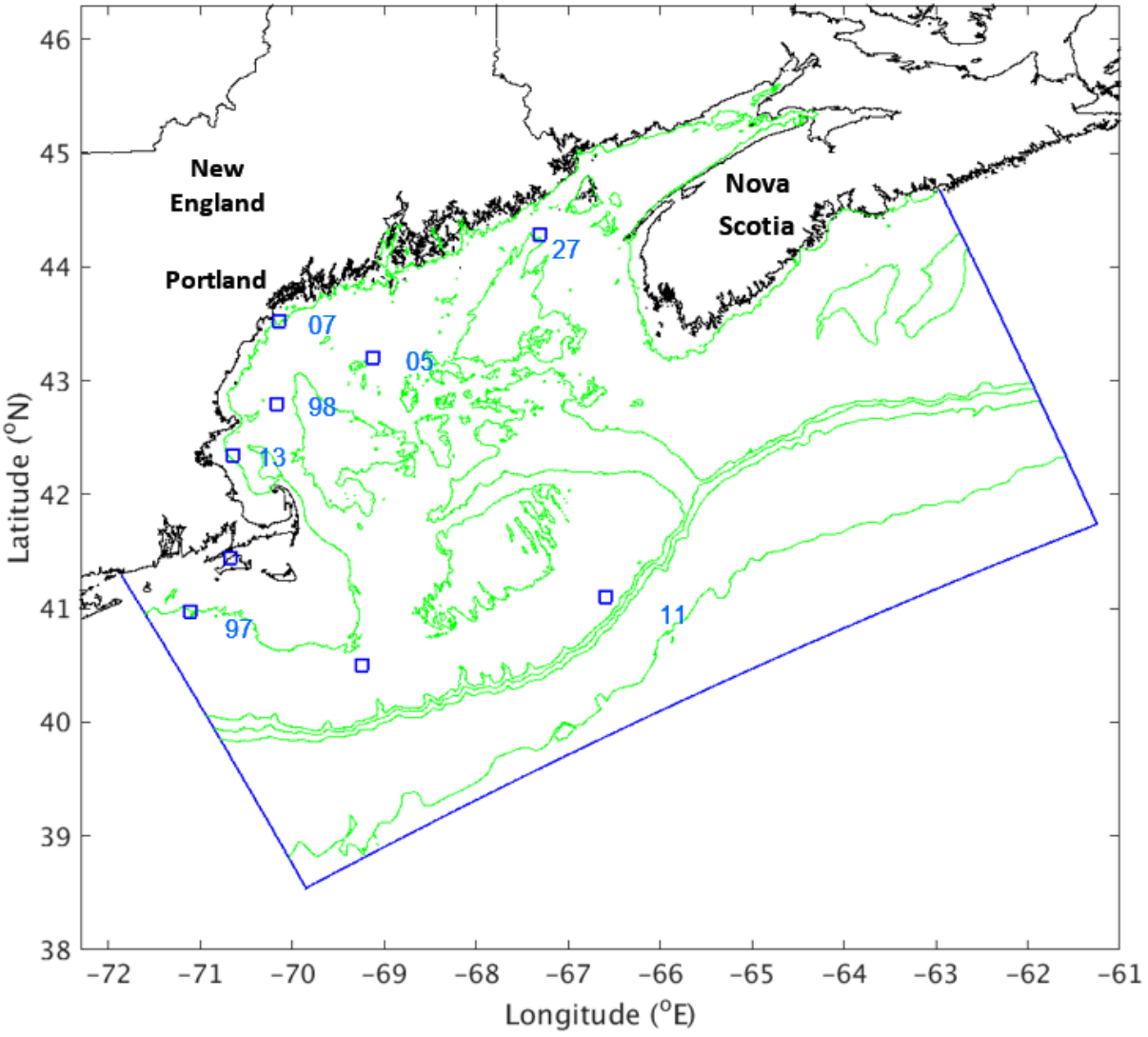

Figure 5. Map of NDBC buoy locations. The station IDs are labeled with marks where the three leading digits “440” of each ID number are omitted for clarity of illustration.

Table 5. Depths (D) of NERACOOS buoys data used for the hindcast skill assessment for water temperature (T), salinity (S), and current velocity (U) measurements

Station ID	D (m) for temperature	D (m) for salinity	D (m) for current velocity
A01	1, 2, 4 ,20, 50, 51	1, 20, 50	10, 22, 34, 46
B01	1, 2, 4, 20, 50	1, 20, 50	18, 30, 42
E01	1, 2, 4, 20, 50	1, 20, 50	18, 30, 42, 54, 66
F01	1, 2, 20	1, 20, 50	14, 26, 38, 50, 62, 74
I01	1, 2, 20, 50	1, 20, 50	14, 26, 38, 50, 62
M01	1, 2, 2.8, 20, 50, 150, 200	1, 20, 50,200	34, 58,82, 106, 130, 154, 178, 194
N01	1, 2, 20, 50, 100, 150,180	1, 20, 50,100, 150, 180	24, 48, 72, 96, 104, 128, 152

4. CONSTANT DENSITY TIDAL SIMULATIONS

4.1. Model Run Setup

The constant density tidal only simulation was forced with the harmonic constants of both tidal water level and current on the model grid open ocean boundary (see Chapter 2). The forcing data were calculated using the tidal and current harmonics from the TPXO 8.0-Atlas tidal database developed at the Oregon State University (Egber and Erofeeva, 2002). The database has a horizontal resolution of 1/30°. We chose the eight most prominent tidal constituents (M_2, S_2, N_2, K_2, K_1, O_1, P_1, and Q_1) in the area as the tidal forcing. The harmonic constants of each constituent were interpolated onto the GoMOFS grid. The magnitudes of both tidal amplitude and phase were adjusted to optimize the model-data agreement at the water level stations (Table 1). The adjustments were made through a trial-and-error procedure. Multiple model runs were conducted; the results from each run were compared with observational data and tidal harmonic forcing data on the model's open ocean boundary were adjusted accordingly to optimize the model-data agreement. In quantitative terms, the amplitude was altered by −7.0 cm for M_2, −1.5 cm for S_2, −0.5 cm for N_2, 1.0 cm for P_1, and 3.0 cm for K_1. The phase was altered by 8.0 degrees for M_2, 2.0 degrees for S_2, 6.0 degrees for N_2, 6.0 degrees for K_2, 8.0 degrees for P_1, and 10.0 degrees for K_1. Note that the amplitude forcing data of K_2, O_1, and Q_1 remained unchanged, and the phase forcing data of O_1 and Q_1 remained unchanged.

To evaluate the model setup, a 200-day tidal simulation was conducted beginning from the still water state. We discarded the model output from the first 17 days (the time required to spin-up and reach the equilibrium state) and analyzed both the water level and current outputs for the remaining six months (183 days). The skill assessment results are presented in the following sections.

4.2. Results

Co-tidal and Co-range Fields Figure 6(a) - (h) show the model simulated co-tidal and co-range fields of the M_2, S_2, N_2, and K_1 tides, respectively. For all four constituents, the pattern and magnitude of both the co-tidal and co-range fields demonstrate favorable agreement with those derived from either observations (Moody et al. 1984) or numerical simulations (Yang and Myers, 2007; Chen et al, 2011). The fields exhibit significant spatial variability throughout the model domain and the features of co-oscillation tides are represented as usually observed over marginal seas and bays. Tides in the Gulf are driven by those coming from the open ocean. The co-tidal lines are well aligned around the Gulf entrance that faces the eastern, southern, and western boundaries of the model domain.

The tidal amplitudes are significantly amplified inside the Gulf. For instance, the M_2 amplitude increases from about 0.4 m near the open ocean boundary to nearly 2 m near the entrance to the Bay of Fundy (Figure 1) to around 6 m in the upper Bay. The extreme amplification of the upper Bay is due to the tidal resonance effect created by the specific geometric and bathymetric features of the Gulf of Maine. Tides over Georges Bank and the Nantucket Shoals appear to be rather weak

due to the intense energy and momentum dissipations caused by bottom-friction (Yang and Myers, 2007).

Model-data Comparison Table 6 lists station IDs, magnitudes of the harmonic constants derived from observations, model results, and the corresponding model-data difference at 24 CO-OPS water level stations (Table 1). To illustrate the model skill, Figure 7 shows the scatter plots of the model-data amplitudes (plots (a), (c), (e) and (g)) and phases (plots (b), (d), (f), and (h)) of the four most prominent constituents, M_2, S_2, N_2, and K_1 at the 24 stations. The model-data discrepancy lies within the ten-percent lines for nearly all stations.

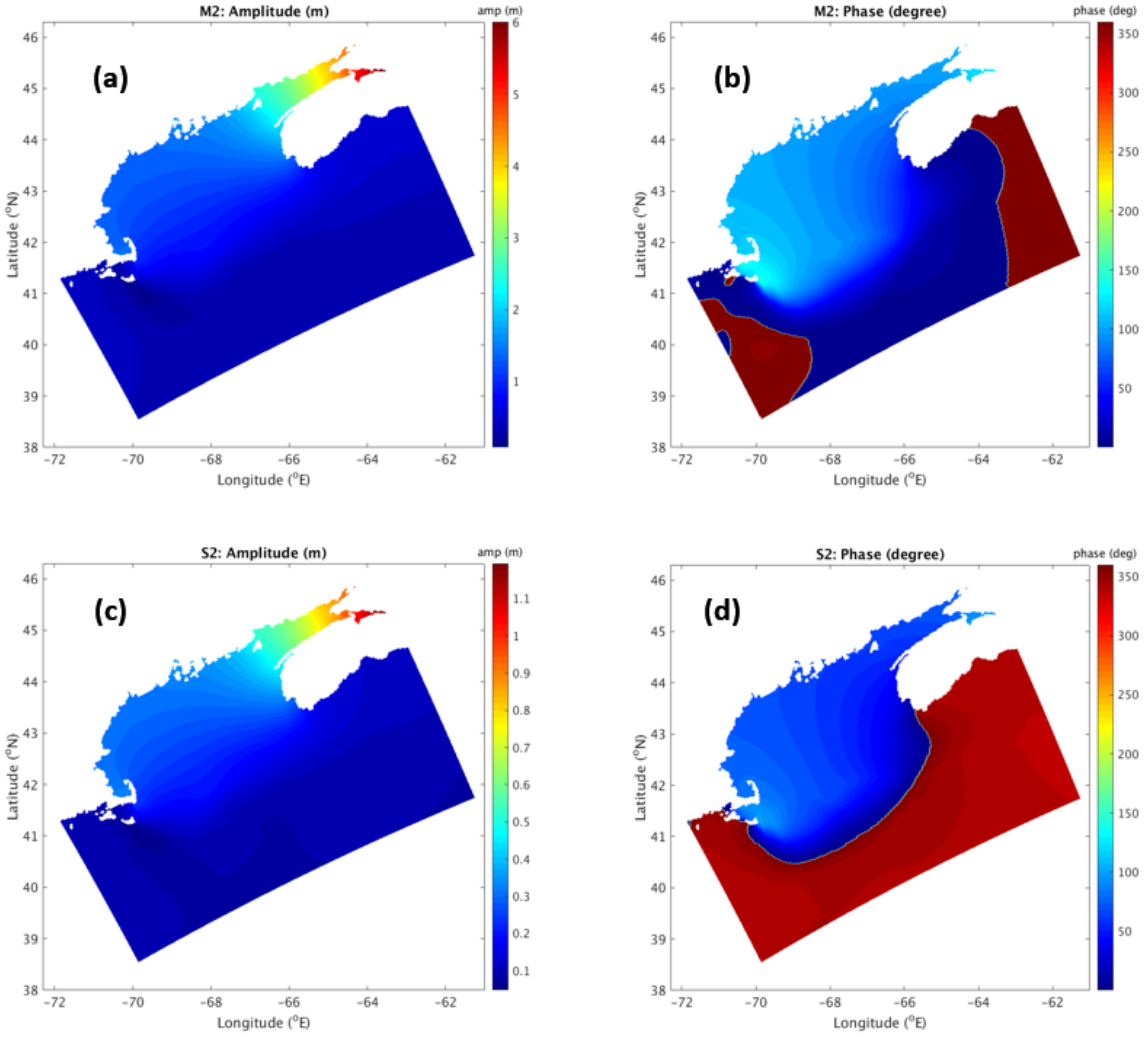

Figure 6. Modeled co-amplitude and co-phase maps for M2, S2, N2, and K1, respectively.

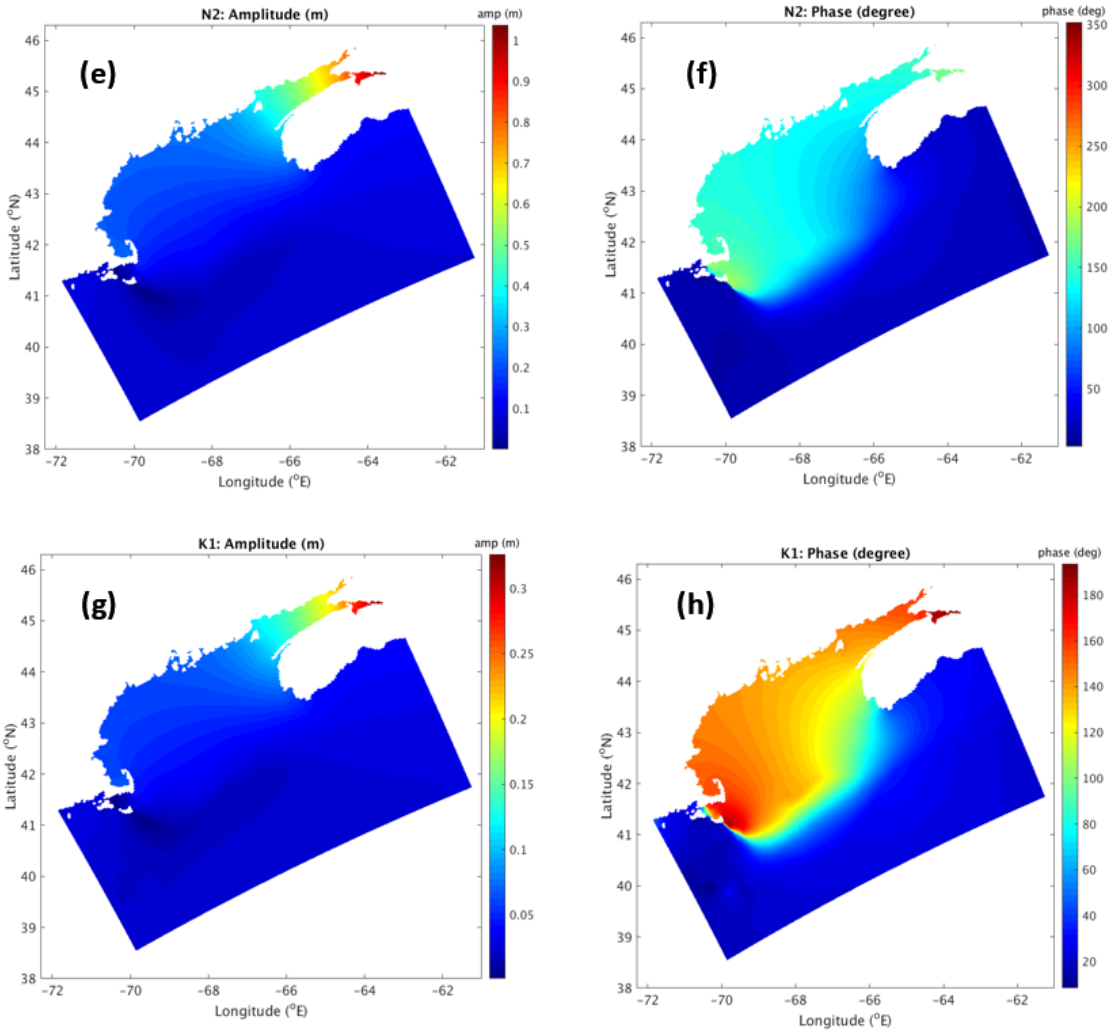

Figure 6. (Continued)

Over the 24 stations, the averaged absolute model-data difference of the tidal amplitude are 3.8, 1.5, 1.1, and 0.4 cm for M_2, S_2, N_2, and K_1, respectively. The corresponding quantities for tide phase are 2.3, 4.3, 2.5, and 2.6 degrees. The tidal simulation produced favorable model-data agreement with respect to both amplitude and phase.

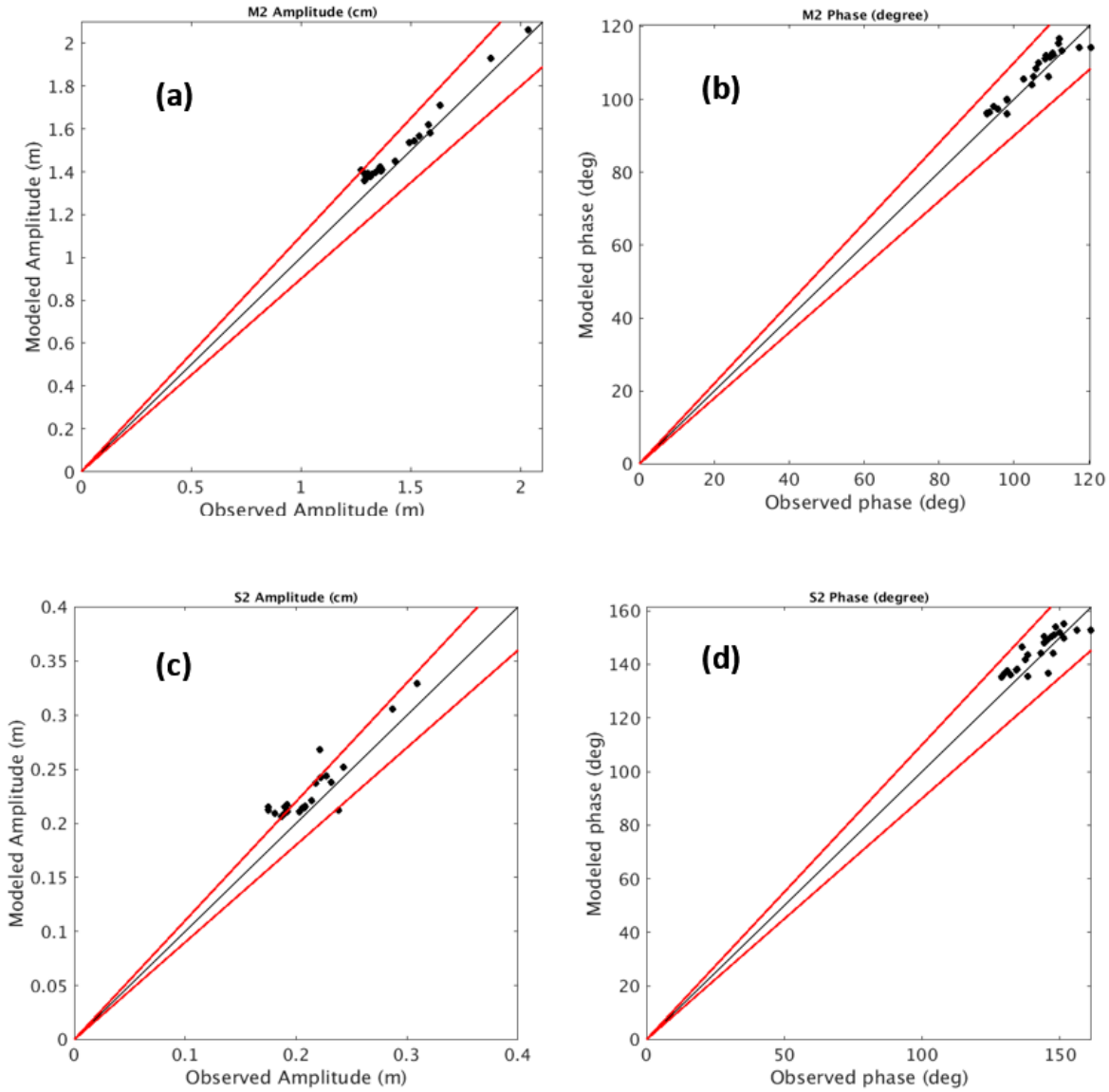

Figure 7. Scatter plots of the tidal harmonic constants (amplitudes and phases) of the M2, N2, S2, and K1 constituents between model results and observations. The red lines on each plot outline the ten percent deviation from the perfect model-data match.

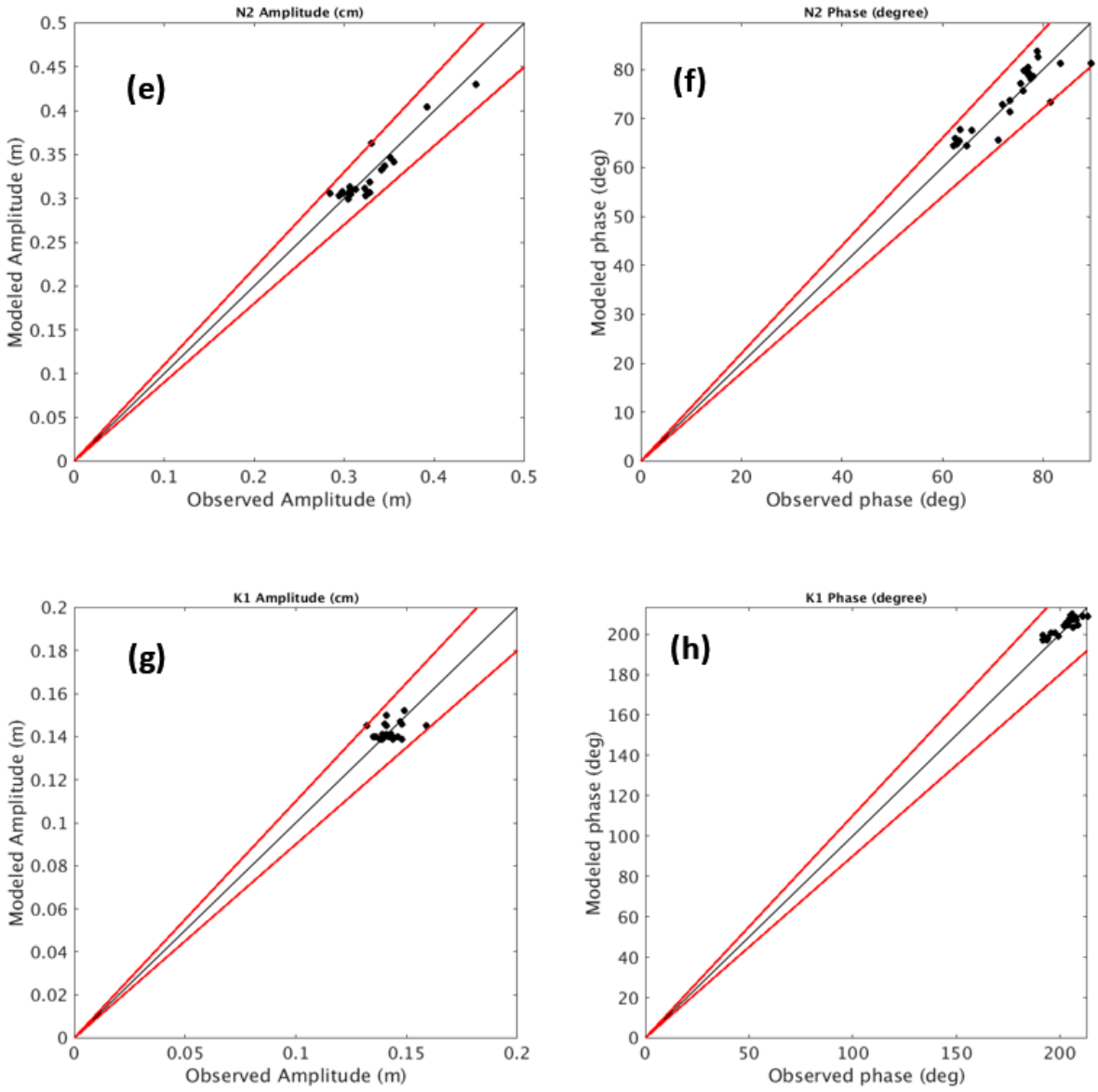

Figure 7. (Continued)

Table 6. The model-data comparison of harmonic constants, amplitude and phase, for the M_2, S_2, N_2, and K_1 constituents. The three values in each cell between columns 2 and 8 represent the observed value, the model result, and the model-data difference.

Station ID	M_2 amplitude (cm)	M_2 phase (degree)	S_2 amplitude (cm)	S_2 phase (degree)	N_2 amplitude (cm)	N_2 phase (degree)	K_1 amplitude (cm)	K_1 phase (degree)
8411250	186.2,183.5,-2.7	92.9,95,2.1	28.7,29.5,0.8	129.8,136.1,6.3	39.2,41.3,2.1	62.8,64.1,1.3	14.1,15,0.9	193.7,195.8,2.1
8411060	203.4,206.4,3	93.4,96.3,3	30.9,32.9,2	131,137.5,6.5	44.6,43,-1.6	63.3,65.5,2.2	14.9,15.2,0.3	191.9,197,5.1
8412581	163.1,171.2,8.1	98.2,96,-2.2	22.1,26.8,4.7	138.4,135.6,-2.8	33,36.3,3.3	64.8,64,-0.4	14.7,14.7,0	192.8,197.6,4.8
8413320	158,154.6,-3.4	92.9,94.6,1.7	24.3,24.4,0.1	128.8,134.3,5.5	35.1,35.4,0.3	62.3,63.4,1.1	14,14.6,0.6	194.3,196.7,2.4
8413825	154,149.9,-4.1	95.6,96.6,1	22.2,23.6,1.4	132.1,136,3.9	34.5,34.5,0	71.2,65.3,-5.9	15.9,14.5,-1.4	199.2,198.1,-1.1
8414249	151.7,147.2,-4.5	94.6,96.6,2	23.2,23.1,-0.1	145.8,135.8,-10	34.1,34,-0.1	62.5,65.2,2.7	13.2,14.5,1.3	191.9,198.2,6.3
8414721	158.9,151.3,-7.6	98.2,99.4,1.2	22.7,23.7,1	134.5,138.5,4	35.5,35.1,-0.5	63.5,67.9,4.4	14.8,14.7,-0.1	195.9,200,4.1
8414888	149.4,146.7,-2.7	98.4,97.9,-0.5	21.6,23,1.4	133.9,136.9,3	34.3,34.1,-0.2	66.5,66.5,0	14.3,14.6,0.3	199.1,199.4,0.3
8417177	127.3,134.4,7.1	104.8,101.8,-3	19,20.9,1.9	137.6,140.5,2.9	29.8,31.5,1.7	73.4,70,-3.4	14.3,14.2,-0.1	206.4,201.9,-4.5
8418150	136.5,140.4,3.9	102.5,105.5,3	20.6,21.4,0.8	138.5,143.6,5.1	30.6,30.8,0.2	72,72.9,0.9	14.1,14.1,0	202.2,204.2,2
8418445	128.4,133,4.6	109.1,103.6,-5.5	17.5,20.6,3.1	147.5,142.3,-5.2	28.4,31.2,2.8	81.5,71.8,-9.7	14,14.1,0.1	208.8,203,-5.8
8418606	130.4,132.9,2.5	105.3,103.8,-1.5	19.2,20.6,1.4	143.1,142.5,-0.6	29.9,31.2,1.3	73.5,72,-1.5	14.6,14.1,-0.5	204.1,203.1,-1
8423898	131.4,137.6,6.2	105.9,108.4,2.5	18.1,20.9,2.8	136.2,146.5,10.3	29.4,30.3,0.9	76.1,75.6,-0.5	13.5,14,0.5	203.3,205.8,2.5
8441551	128.8,129.6,0.8	106.6,107.3,0.7	18.7,20,1.3	144.2,146.2,2	30.4,30.6,0.2	75.5,75.4,-0.1	14.4,14,-0.4	204.9,205,0.1
8442645	130.1,137.4,7.3	108.3,111.1,2.8	19,20.9,1.9	145.6,149.3,3.7	32.4,30.3,-2.1	77.6,78.2,0.6	14.8,13.9,-0.9	206.2,207.2,1
8443187	133.8,139.5,5.7	109.7,111.5,1.8	23.8,21.2,-2.6	151.5,149.8,-1.7	32.8,30.7,-2.1	78.1,78.6,0.5	13.5,14,0.5	208,207.4,-0.6
8444162	132.3,132.9,0.6	108.6,109.5,0.9	20.3,20.6,0.3	144.4,148.5,4.1	30.5,31.4,0.8	77,77.5,0.5	13.9,14.1,0.2	204.6,206.1,1.5
8445138	129.6,137.4,7.8	110.3,112.7,2.4	19,20.9,1.9	147.8,151,3.2	29.4,30.3,0.9	76.2,79.7,3.5	13.9,13.9,0	205.7,208,2.3
8444525	136,134.7,-1.3	110.6,110.1,-0.5	20.7,20.9,0.2	147.1,149.2,2.1	31.3,31.8,0.5	77.2,78.2,1	13.9,14.1,0.2	205.8,206.5,0.7
8446009	130.3,132.2,1.9	112.8,110.9,-1.9	19.2,20.5,1.3	150.1,149.9,-0.2	30.7,31.2,0.5	77.1,78.9,1.8	13.8,14,0.2	207.6,206.8,-0.8
8446121	136.7,136,-0.7	112,114.5,2.5	17.5,21.1,3.6	151.3,153.8,2.5	32.3,32.1,-0.2	78.8,82.5,3.7	13.6,14.2,0.6	206.1,208.6,2.5
8446166	136.2,136.4,0.2	120.4,113.1,-7.3	19.2,21.2,2	161.4,152.3,-9.1	30.6,32.2,1.6	89.5,81.1,-8.4	14.2,14.2,0	213.2,208,-5.2
8446493	135.5,135.7,0.2	117.4,112.8,-4.6	20.8,21.1,0.3	156.3,152,-4.3	30.6,32,1.4	83.5,80.8,-2.7	14,14.2,0.2	210.9,207.8,-3.1
8447241	142.9,139,-3.9	111.8,113.2,1.4	21.4,21.6,0.2	148.5,152.4,3.9	32.8,32.8,0	79,81.2,2.1	13.9,14.3,0.4	205,207.9,2.9

5. SYNOPTIC HINDCAST SIMULATIONS

This chapter describes the skill assessment results of hindcast simulations. The simulations span the modeling period from 1 January 2012 to 30 December 2012. It started from a still water state with the T/S fields initialized with the G-RTOFS nowcasts. Following an initial 5-day ramping up, the model run continued for another 10 days to ensure that an equilibrium state was reached. The time series of various ocean state variables including water level, currents, and T/S, were recorded at 6-minute intervals from the 15th day to the end of the hindcast period. The time series then underwent skill assessment using the NOS standard skill assessment software (Zhang et al, 2006).

The model time series of water level, currents, temperature, and salinity were compared with the observed data (Chapter 2). The resulting values of the two key model skill parameters, RMSE and the central frequency (CF), are discussed in the following. CF represents the fraction (percentage) of the model errors that are less than some prescribed criteria value for RMSE. The NOS standard prescribes the criteria value as 0.15 cm for water level, 0.26 m/s for current speed, 22.5 degrees for the current phase, 3.0 °C for water temperature, and 3.5 psu for salinity. The standard prescribes as well a constant value of CF equal to 90% for all the above listed ocean state parameters. The present skill assessment results demonstrate that the hindcast performance met the above criteria.

5.1. Water Levels

The model and observed water level time series at six NOS/CO-OPS stations (Table 1) were compared (Figure 8).

5.1.1. Total Water Level

Figure 8(a) - (f) display the model and observed water level time series at each station. For the sake of clarity, each plot shows only a portion of the one-year data, from October 1, 2012 through early November 2012. The model results demonstrate favorable agreement with the observations in terms of both amplitude and phase.

Figure 9(a) and (b) display the RMSE and CF, respectively. The RMSE ranges from 0.09 m (Station ID 8418150, Portland, ME) to nearly 0.13 m (Station ID 8411060, Cutler Farris Wharf, ME). The CF ranges from 76.2% (Station ID 8411060, Cutler Farris Wharf, ME) to 89.6% (Station ID 8418150, Portland, ME). With respect to the RMSE and CF, the hindcast demonstrated better skill at stations near the central western Gulf coast than at stations along the Massachusetts coast and the northern Maine coast.

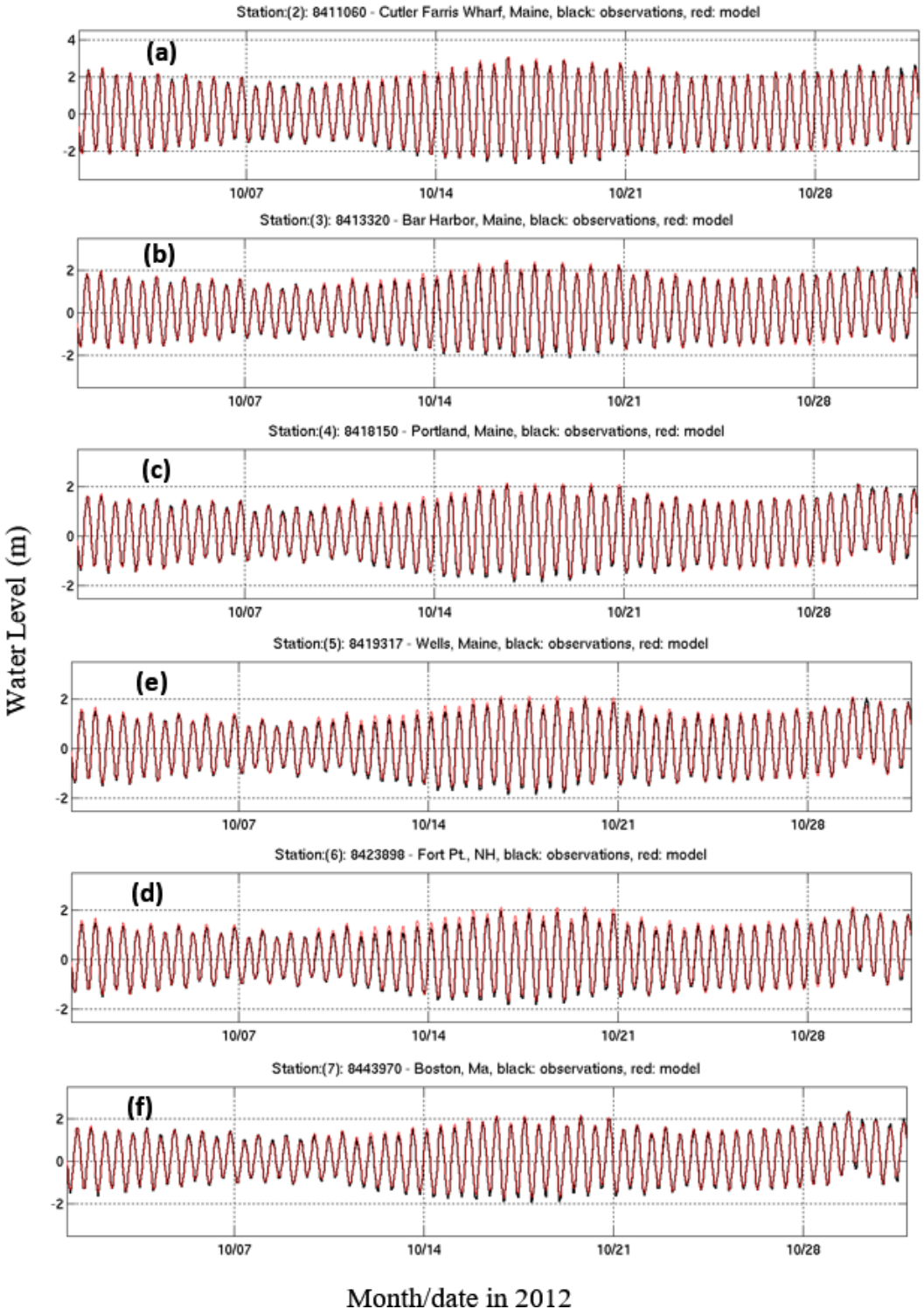

Figure 8. Comparison of hindcasts vs. observed water level time series at six CO-OPS water level stations (Table 1). The red and black lines represent the model hindcasts and observations, respectively.

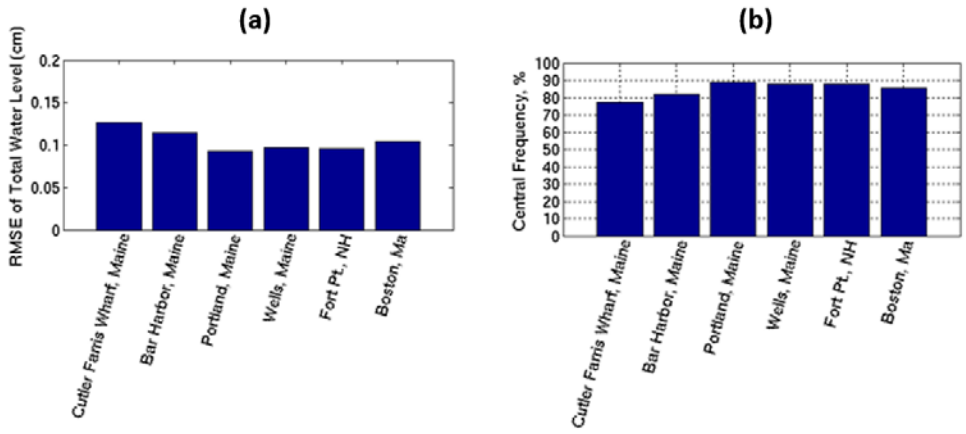

Figure 9. Skill assessment results of the tidal water level. (a) RMSE and (b) CF.

5.1.2. Subtidal Water Level

To investigate the model performance on the subtidal water level, the total water level time series were filtered using a 30-day low-pass Fourier Transform filter.

Figure 10(a) - (f) show both the model and observed subtidal water level time series after applying the filter to the total water level data. The model results demonstrate favorable agreement with the observations during both the event-free period ending in late October, and the event period of late October through early November. For instance, Figures 5.3(a) and 5.3(f) indicate that the model successfully reproduced the water level setup at stations 8423898, and 8443970 in early November. At some stations, such as 8419317 and 8423898 (Figures 5.3(d) and 5.3(e), respectively), the model slightly over-predicted the water levels in mid-October. The model RMSE ranges between 4.4 cm and 5.8 cm at the six stations.

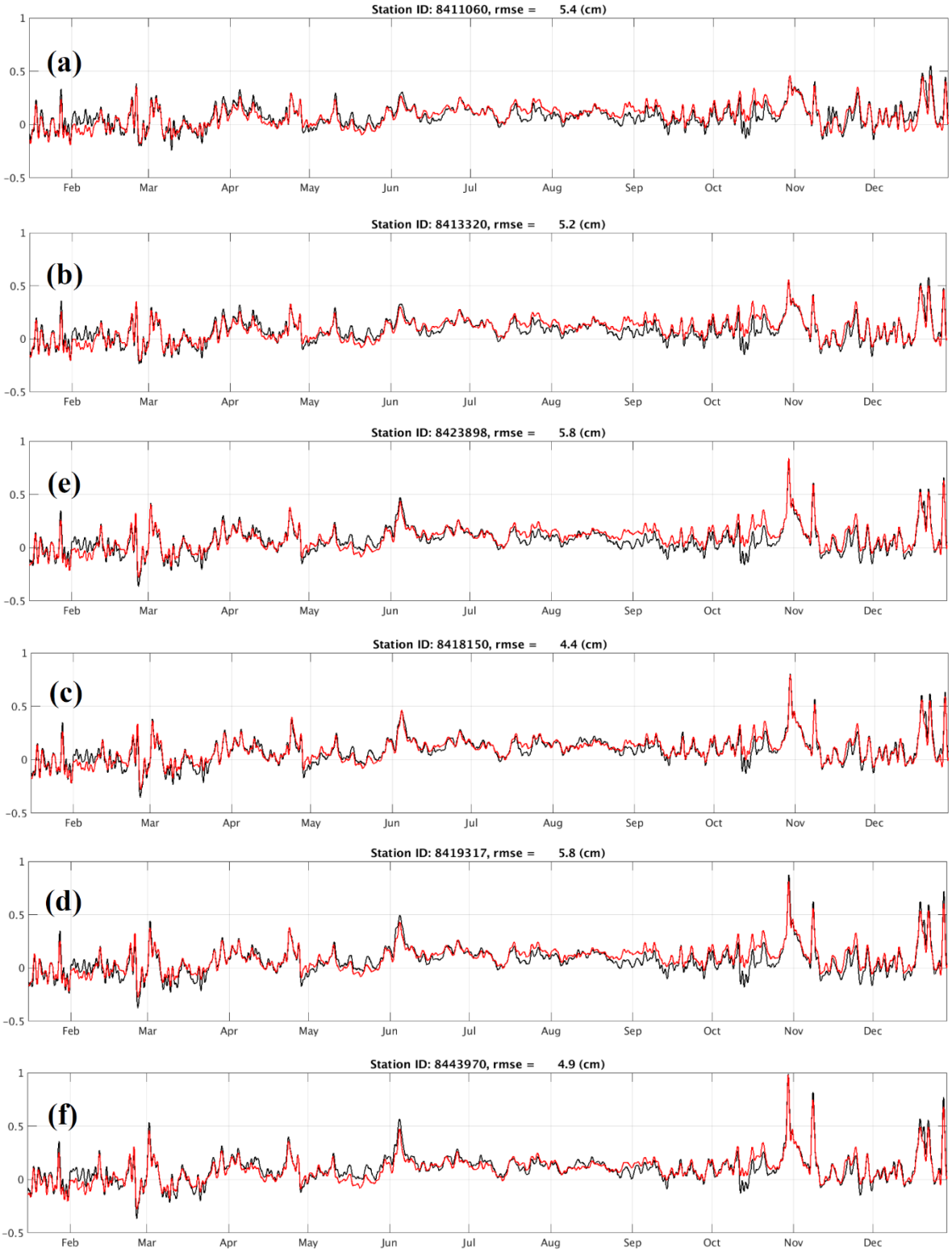

Figure 10. Subtidal water levels at six CO-OPS water level stations (Figure 1). The red and black lines represent the model hindcasts and observations, respectively. The six plots are for stations (a) 8411060, (b) 8413320, (c) 8418150, (d) 8419317, (e) 8423898, and (f) 8443970.

5.2. Currents

Figure 11 shows the current speed and direction time series of both the model and observed data at three measurement depths (10 m, 22 m, and 46 m) at buoy A01 (Figure 4 and Table 3.5). The model results demonstrate close agreement with the observations. Specifically, the model favorably reproduces current speed and direction during several prominent events with respect to both their timing and amplitude. As shown in Figures 5.4(a) and 5.4(c), the events took place at the end of March, early June, early and mid-November, and late December. They appear to be more intense in the shallow layers (Figures 5.4(a) and 5.4(c)) than in deeper layers (Figure 11(e)). Comparison of wind time series vs. current time series indicate that the enhanced current speeds result from the intensified wind stress during these events.

Following the NOS skill assessment standards, the model performance of water current were evaluated in terms of the current speed and phase, respectively. Figure 12 (a) and (b) display the RMSE of the current speed and phase, respectively. For the current speed, the RMSE ranges from 0.05 m/s at station E-66m to about 0.20 m/s at stations F-74m and N-24m. CF were mostly greater than 95% and lay between 80% and 90% at stations F-74m and N-24m. At buoys stations A, B, E, F, and M, RMSEs ranged between less than 2 degrees to 10 degrees and CFs were all above 95%. At station N01, RMSE was between 15 cm/s and 17 cm/s and CF was around 85% at all depths.

Note that station N01 demonstrated significantly less favorable model skills than the other stations. This might be related to the complex hydrodynamics surrounding the station location. Station N01 is positioned along the Northeast Channel (Figure 4). The channel has a sill depth of 230 m and is the major pathway for the water mass exchange between the Gulf and the open ocean. The deep ocean water flows into the central Gulf at depth and the Scotian water flows across the channel in the near surface layer. The channel also serves as a major route for tidal energy to propagate into the Gulf. The combined subtidal and tidal current may reach a speed of well over 1 m/s. In contrast, the hydrodynamics in other areas of the Gulf appear to be much less complex. The complex hydrodynamics in the channel pose a more serious challenge to the realistic reproduction of local hydrography than elsewhere and contribute to the greater model error at Station N01.

We further examined model performance in reproducing subtidal currents. Figure 13 displays the (u, v) components of the modeled and observed subtidal time series at three measurement depths (10 m, 22 m, and 46 m) at buoy A. The subtidal model output was extracted from the total water level by filtering the model output with a 30-hour low-pass Fourier Transform filter. The hindcast simulation successfully reproduced the events taking place in early June and early to mid-November. During these events, the currents appeared to be more intense in shallow layers (at 10 m and 22 m) than in deeper layers (at 46 m). Comparison of the time series between the winds and the currents indicate that the enhanced currents speeds resulted from the intensified wind stress during the events.

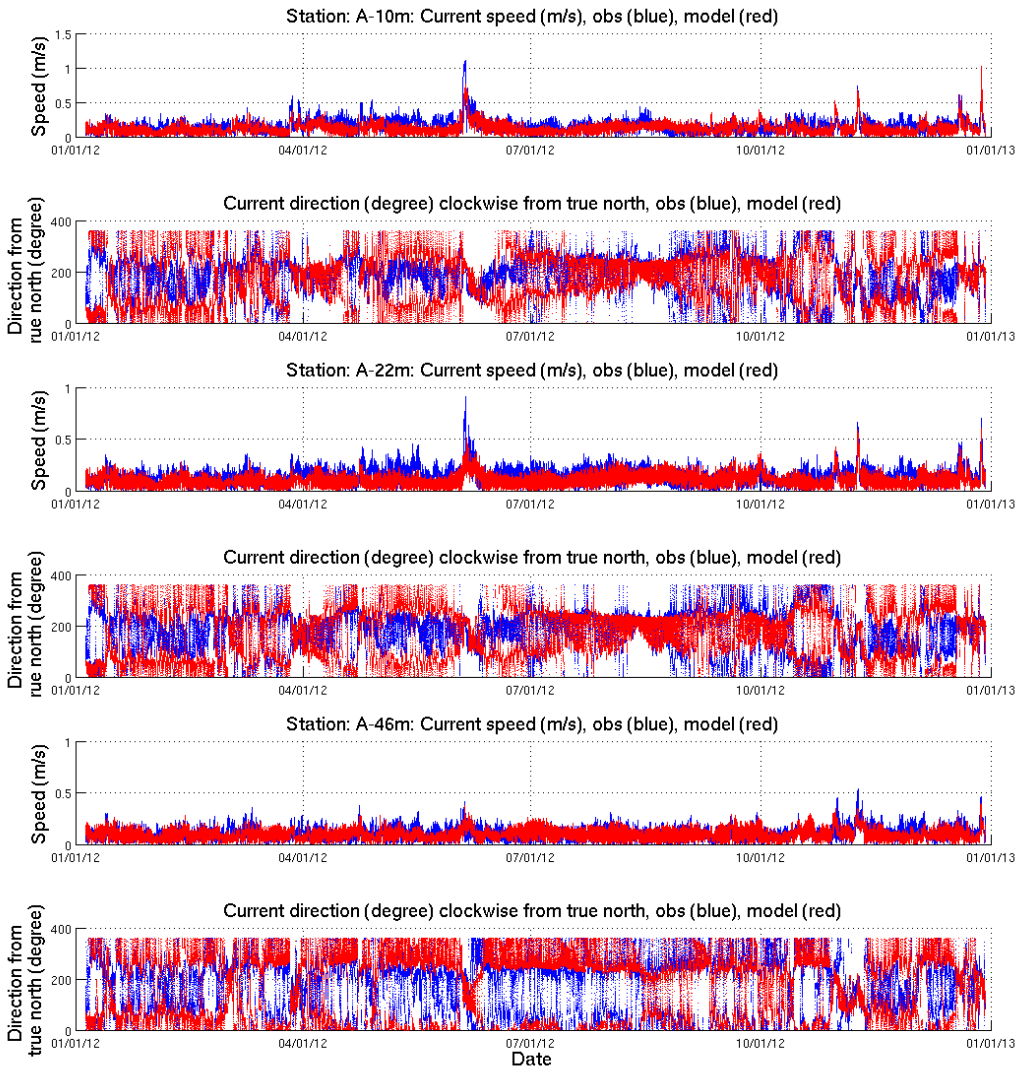

Figure 11. Comparison of the model hindcasts (red lines) and the data (blue lines) time series of the currents speed and direction at the NERACOOS buoy station A. The plots correspond to three depths, 10 m (a and b), 22 m (c and d), and 46 m (e and f), respective.

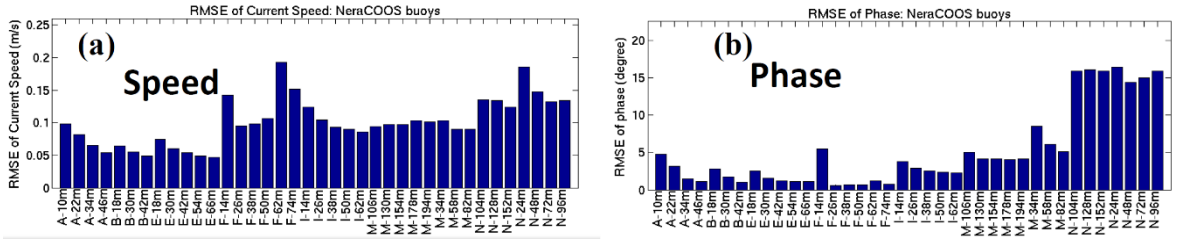

Figure 12. Skill assessment results of the current speed and phase. (a) RMSE of speed and (b) RMSE of phase.

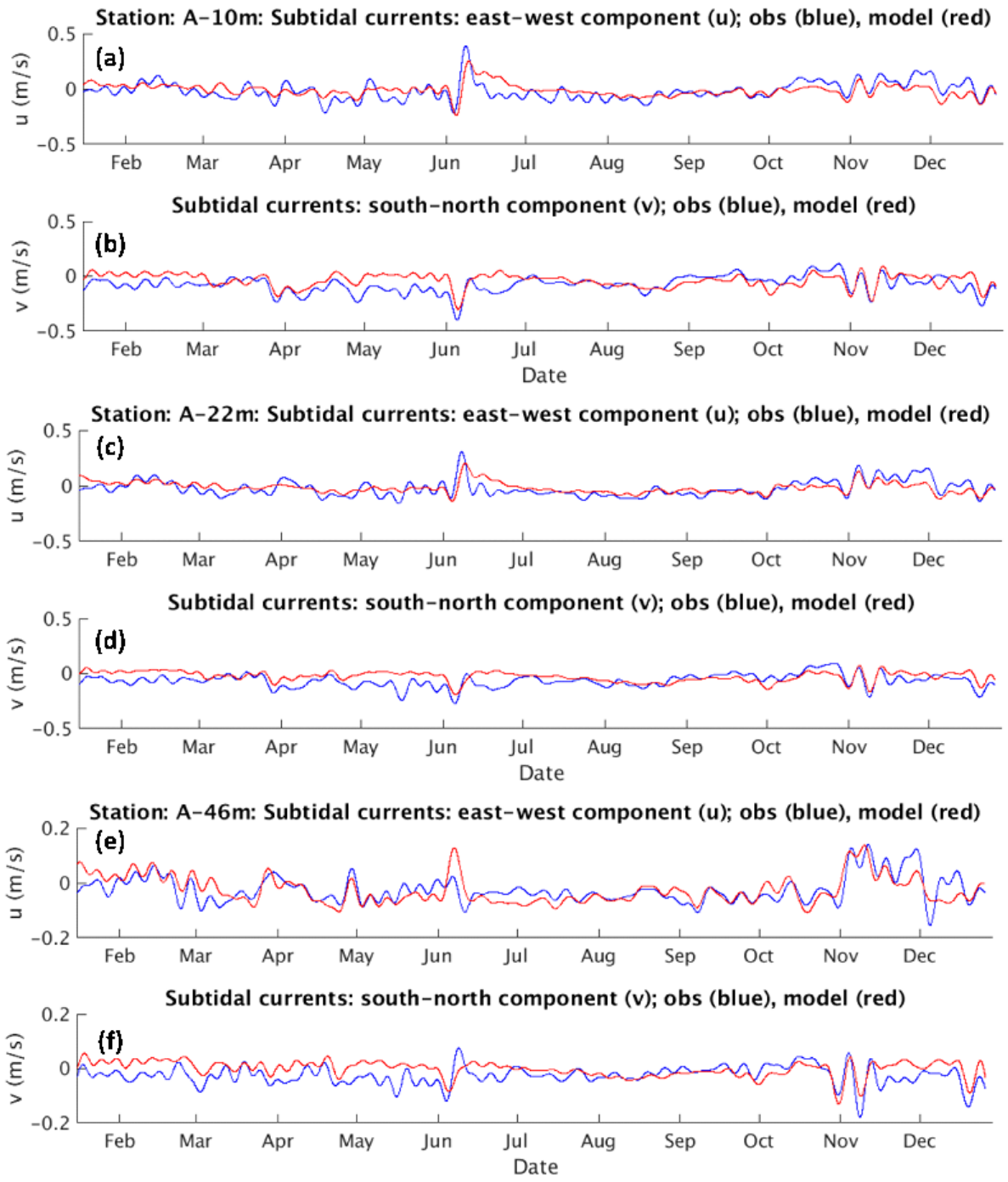

Figure 13. Comparison of the model hindcasts (red lines) and the data (blue lines) time series of the current velocity (u, v) at the NERACOOS buoy station A. The station names are denoted with the first letter representing the buoy ID (Table 3.3) and the following digits for the measurement depths. (a) and (b) depict the u and v components at the 10 m depth; (c) and (d) depict the u and v components at the 22 m depth; and (e) and (f) depict the u and v components at the 46 m depth.

5.3. Water Temperature

Skill Assessment Statistics The model water temperature hindcasts time series were compared with the observations at the CO-OPS meteorological stations and the NDBC buoys, and NERACOOS buoys. The model hindcasts demonstrated favorable agreement with the observations. As an example, Figure 14(a)-(e) display both the model and observed water temperature at six depths (1 m, 2 m, 2.8m, 100 m, and 150 m) at the NERACOOS buoy M01. The plots illustrate that the model successfully reproduced both the magnitude and the annual cycle of the temperature. The near surface water temperature varied between 6 °C in the winter and the early spring and 20 °C in the mid-summer. In deeper water, the water temperature remained at a nearly constant value of 9 °C throughout the year. This suggests that a very strong thermocline existed during the summer and completely faded away in the winter.

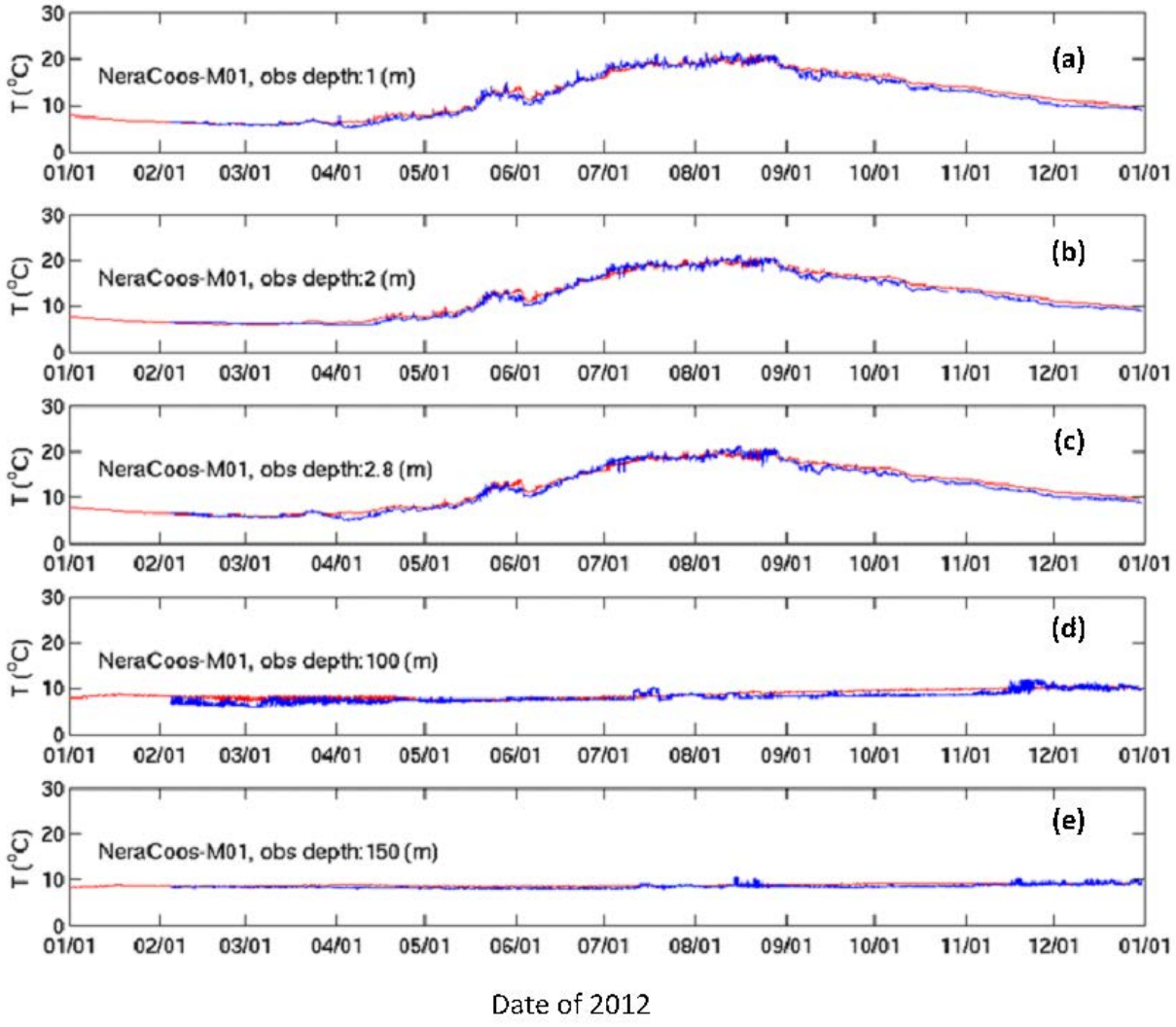

Figure 14. Comparison of the model hindcasts (red lines) and the data (blue lines) time series of water temperature measured at various depths at the NERACOOS buoy M01. The measurement depths are as shown on each plot.

Figure 15 illustrates the skill assessment results with respect to the three sources of observed data: the CO-OPS weather stations (Table 3.2), the NDBC buoys (Table 3.3), and the NERACOOS buoys (Table 3.4). In each figure, the abscissa represents the station ID. The NERACOOS station IDs which appear in Figure 15(e) and 15(f) follow the same naming convention as in Figure 14. Both the CO-OPS data and the NDBC buoy data correspond to the near surface measurements and the NERACOOS data cover both the near surface and in-depth measurements. In addition, the CO-OPS stations were located in the nearshore area whereas the other two data sets (the NDBC and NERACOOS buoys) were located in areas further offshore and extended to the central Gulf and near the shelfbreak area. Therefore, the skill assessment results of the three groups assess the hindcast performance in different hydrodynamic regimes, e.g., nearshore vs. offshore areas as well as at the sea surface vs. the in-depth waters.

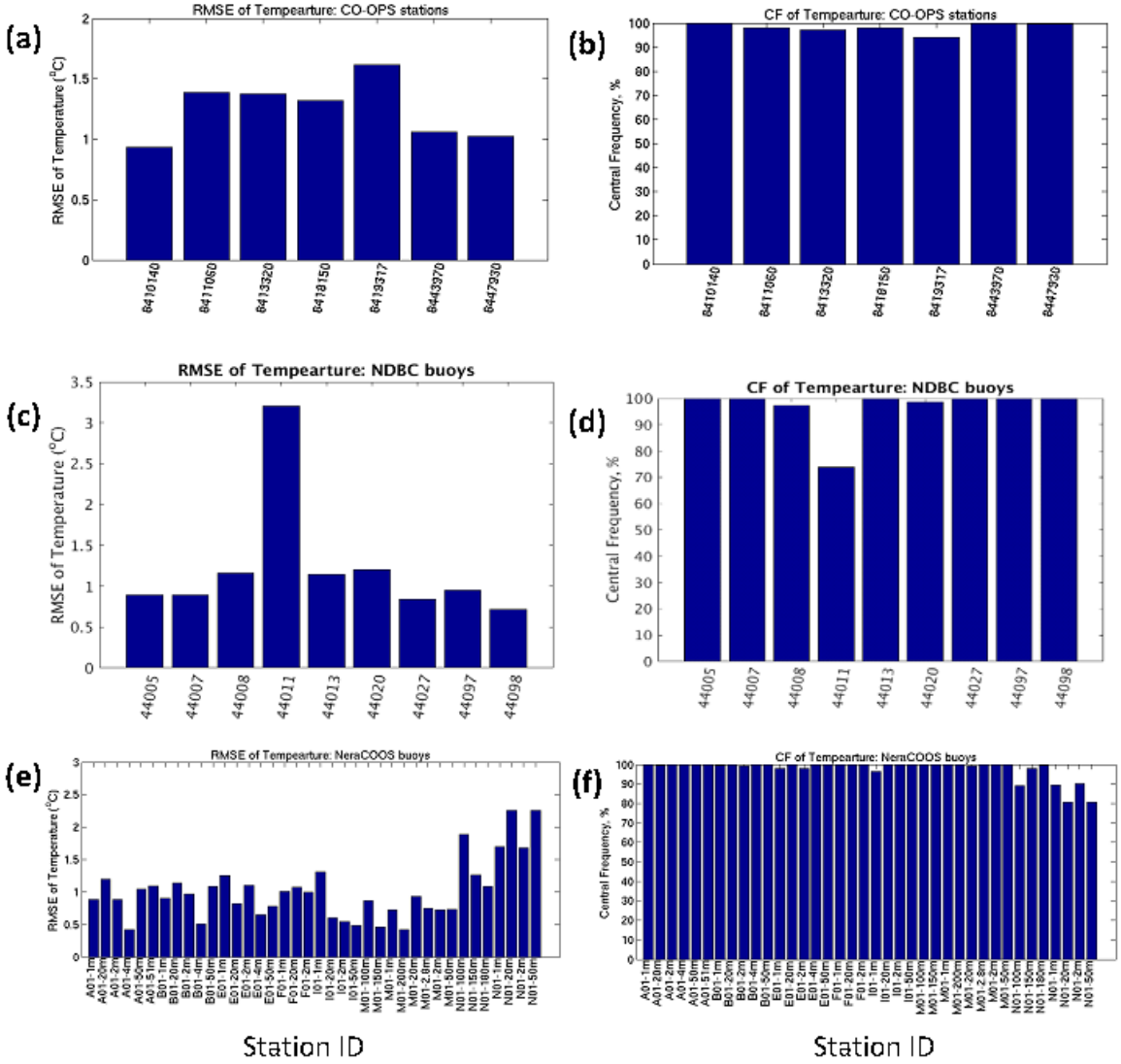

Figure 15. Results of the skill assessment of water temperature hindcasts. The three rows correspond to the three data sources: the CO-OPS weather stations, the NDBC buoys, and the NERACOOS buoys. The two columns correspond to RMSE and CF.

The RMSE at the seven CO-OPS stations ranged from 0.9 ºC to 1.7 ºC and CF was all above 95%. The RMSE at the NDBC stations was between 0.7 ºC and 1.8 ºC except for an outlier of 3.3 ºC at station 44011 (Table 3.3). Correspondingly, CF was above 90% except at station 44011 which had a CF of about 70%. A detailed examination of the observed time series from the station revealed that an abrupt temperature jump of over 2.5 ºC occurred in June 2012. We deemed the jump to be unrealistic and attributed the large RMSE to instrument malfunction.

The RMSE at the NERACOOS stations ranged from less than 1.0 ºC at station M in the eastern Gulf to around 2.3 ºC at station N01 (20m depth and 50m depth). CF was above 90% except at station N01 (20m and 50m) for which CF equaled ~80%. Note that buoy N is located in the NEC (Figure 1). That is close to the GoMOFS southern open ocean boundary. The hydrodynamics there are largely governed by the model's boundary forcing conditions. We attribute the relatively greater RMSE at the two stations to boundary condition errors inherited from the G-RTOFS results.

Monthly Mean The model results demonstrate favorable agreement with the observations in terms of monthly mean. As an example, the left panel in Figure 16 displays the monthly averaged temperature at six depths (1 m, 20 m, 50 m, 100 m, 150 m, and 200) at the NERACOOS buoy M01. The plots illustrate that the model successfully reproduced both the magnitude and the annual cycle of the water temperature. The near surface water temperature varied between 6ºC in the winter and the early spring and 20ºC in the mid-summer. In deeper water, temperature remained at a nearly constant value of 9ºC throughout the year. This suggests the existence of an intense thermocline during the summer which dissipates by winter

The right panel displays the bias and the standard deviation (std) of the monthly averaged model water temperature hindcasts. The bias ranges from near zero to less than 1°C and does not exhibit a trend of seasonal variation. The std ranges between 0.03 and 1.2°C and appear to be greater in summer than in spring and winter. In general, the model std at other buoys demonstrate both similar trends and the similar order of magnitude of seasonal variability.

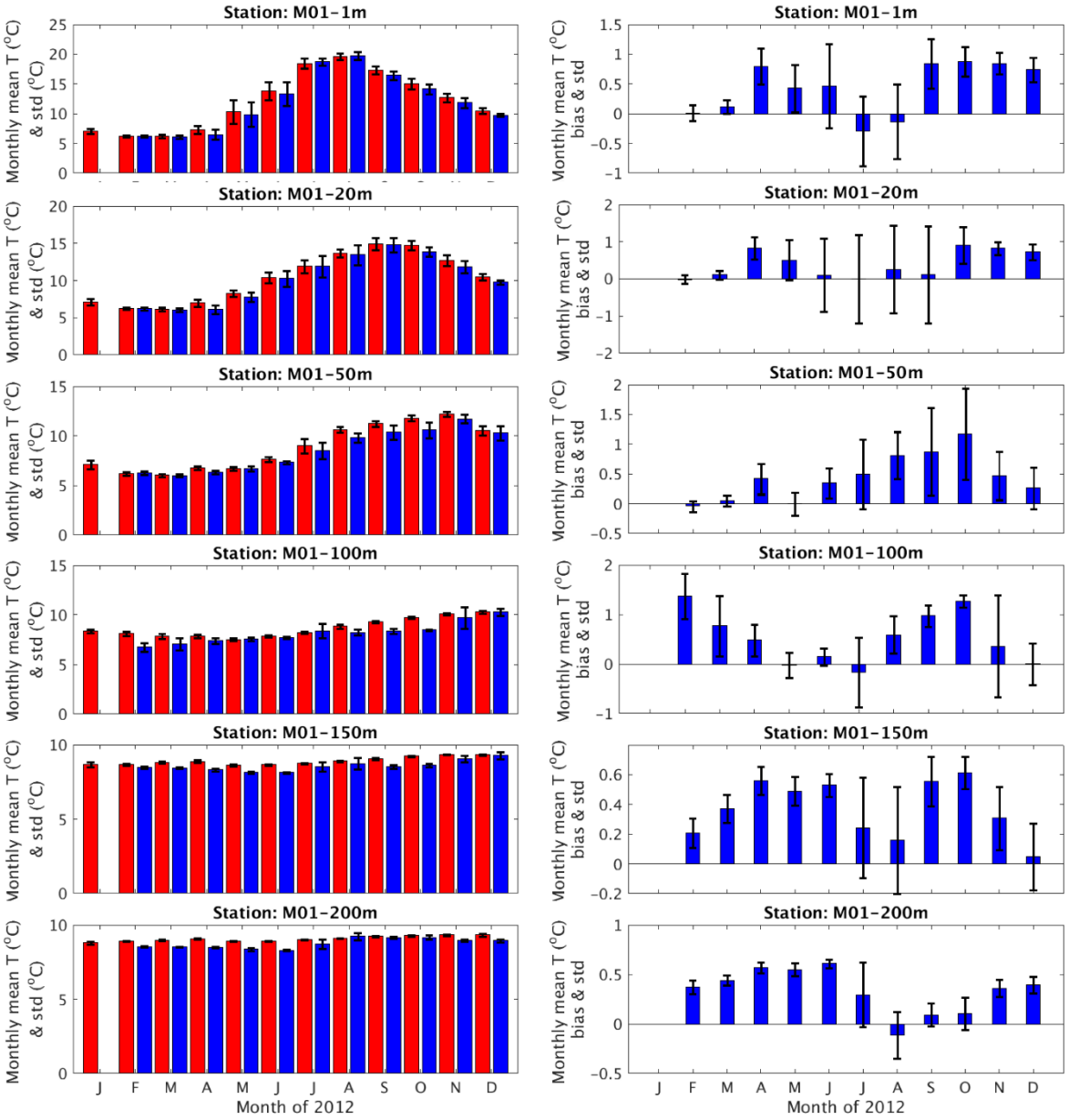

Figure 16. (Left panel) Comparison of the monthly averaged model hindcasts (red bars) and the observed (blue bars) water temperature at the NERACOOS buoy M01. The measurement depths are as shown on each plot. The average observed temperature values do not appear for January of 2012 due to the lack of data. (Right panel) Bias of the modeled monthly mean temperature. The thin lines on top of each bar plot represent the corresponding standard deviations.

5.4. Salinity

Skill Assessment Statistics The model hindcasts of salinity time series were compared with observations at the seven NERACOOS buoys (Table 3). The model hindcasts results demonstrate favorable agreement with the observations. Figure 17 shows the model (red lines) and the observed data (blue lines) time series at buoy A01, shown in Figure 17(a) - (c), and buoy M01, shown in Figures 17(d) - (i). The corresponding observation depths are 1 m, 20 m, and 50 m at buoy A01 and 1 m, 20 m, 50 m, 100 m, 150 m, and 200 m at buoy M01.

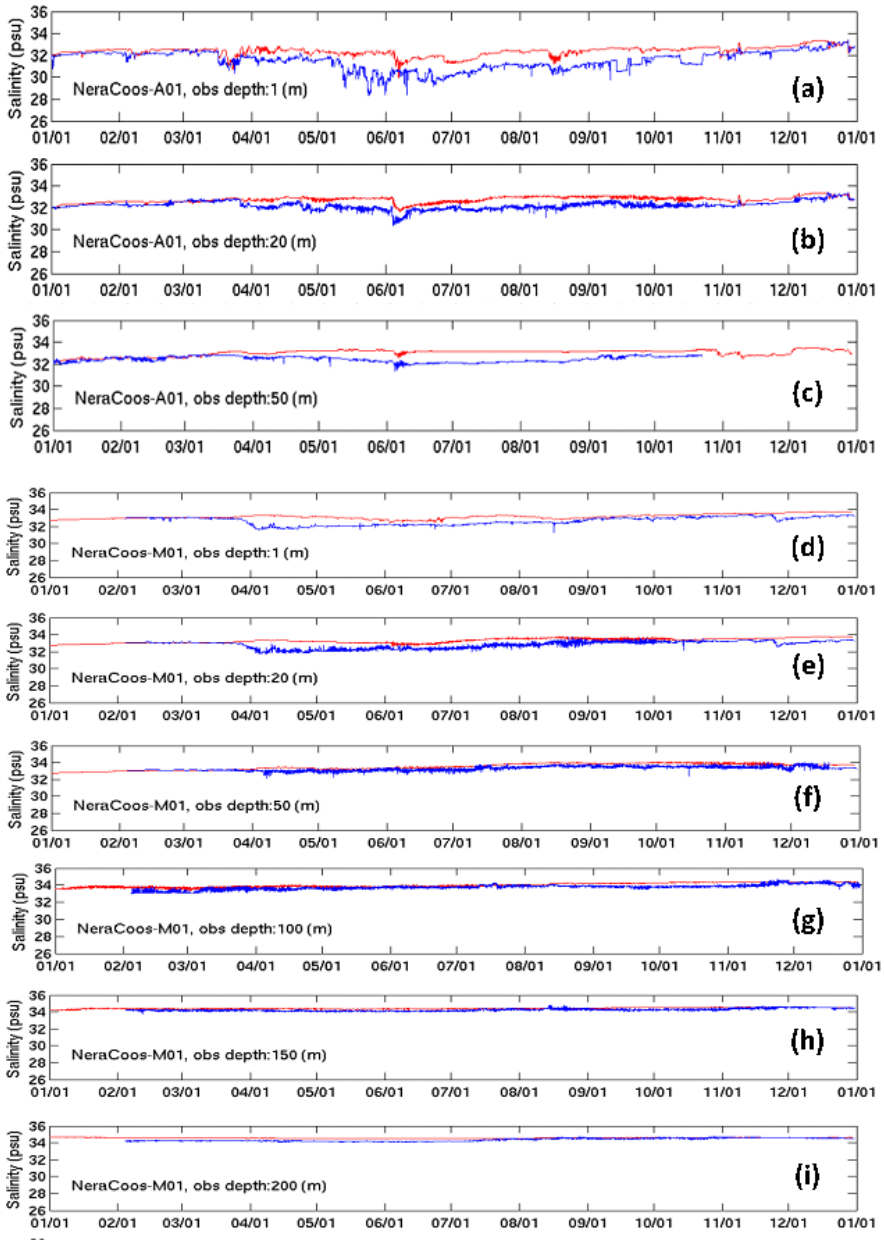

Figure 17. Comparison of the model hindcasts (red lines) and the data (blue lines) time series of salinity at the NERACOOS buoy A01 (plots (a) - (c)) and M01 (plots (d) - (i)). The measurement depths are shown on each plot.

In general, salinity exhibits greater temporal variability near the surface than in deeper water, especially during the late spring, summer, and early fall. This may be attributed to the combined ambient influence of the seasonal fluctuations of river runoff and precipitation. During these periods, the model-data discrepancy appears to be greater than in the winter. For instance, at buoy A01 (Figure 17(a) - (c)), the modeled surface salinity differ from the observations by 1.5 to 2 psu in the summer months, whereas the two exhibit a close match in the winter months. Further offshore at buoy M01 (Figure 7(d)-(i)), the model-data discrepancy appears to be much smaller than at buoy A01. The model showed good agreement with the observations in the fall and winter seasons. Even during the hydrodynamically active spring and summer seasons, the model hindcasts and observations differed by an amount generally less than 1 psu.

Figure 11 displays the RMSE and CF of the salinity skill assessment results. In general, the RMSE ranged from 0.2 psu to 1.5 psu and the CF was close to 100%. At buoys A, B, E, F, I, and M, the RMSE of the near-surface salinity was around 1.0-1.5 psu, whereas the RMSE in the subsurface layer is much smaller, generally less than 0.7 psu. At buoy N, the RMSEs at all three depths (1 m, 20m, and 50 m) were between 1.0 psu and 1.4 psu.

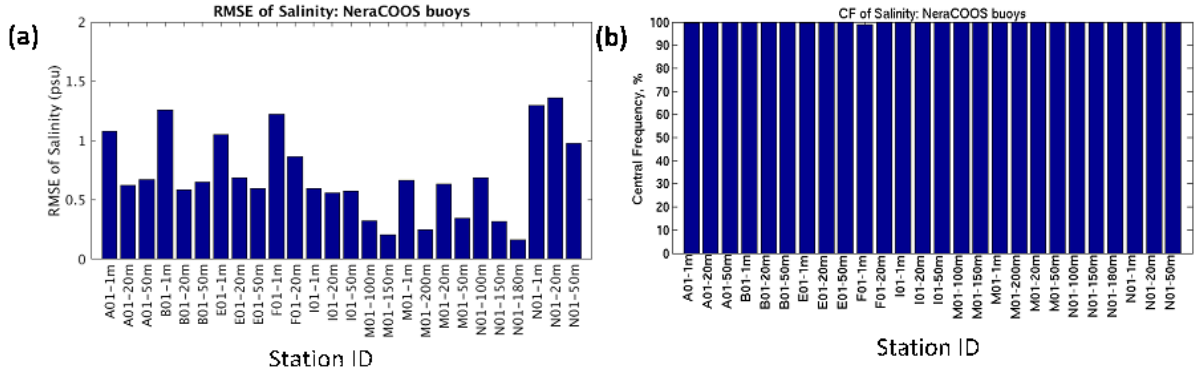

Figure 18. Skill assessment results of salinity. (a) RMSE and (b) CF.

Monthly mean The modeled monthly mean salinity demonstrates favorable agreement with the corresponding observations. For example, Figure 19 shows the comparison of monthly averaged model and observed salinity at buoys A01 and M01. The corresponding measurement depths were 1 m, 20 m, and 50 m at buoy A01 and 1 m, 20 m, 50 m, 100 m, 150 m, and 200 m at buoy M01. The right panel displays the corresponding model bias and std.

In general, salinity exhibits greater temporal variability near the surface than in deeper waters, especially during the late spring, summer, and early fall. The modeled salinity demonstrates a positive bias with a typical magnitude of 0.5-1.0 psu at nearly each station throughout the year. This indicates that the hindcast tended to overestimate the salinity. However, this issue does not seem to be rooted in the specifics of the currently adopted turbulence closure scheme (TCS). In fact, other TCS such as the k-ε, k-ω, and KPP models in the ROMS were tested and they demonstrated similar model skills. Model bias might be attributed to inherent errors of various model forcing data.

Similar to the results for the un-averaged time series, the model-data discrepancy appears to be greater in the summer than in the winter. For instance, at buoy A01, the modeled surface salinity differed from the observations by 1.5 to 2 psu in the summer months, whereas the two exhibited a close match during the winter months. Further offshore, at buoy M01, the model-data discrepancy appears to be much smaller than at buoy A. The model agrees well with the observations in the fall and winter seasons. Even during the hydrodynamically active spring and summer seasons, the model-data differed by less than about 1 psu.

River Effect To examine the impact of the river discharge and rainfall forcing on model salinity, we estimated the correlation coefficient, C_{SP}, between the sea-surface salinity (SSS) and the precipitation rate. We then calculated the correlation coefficient, C_{SR}, between the SSS and the discharge rate from the nearest river to each NERACOOS station. The magnitude of C_{SP} was less than 0.06 at all stations. This indicates that at the NERACOOS stations, the rainfall plays a minor role in determining the SSS compared with other forcing factors or ambient conditions.

C_{SR} was −0.42 and −0.46 at Stations B and F, respectively, and was much less significant ($|C_{SR}| < 0.05$) at the other stations. Note that Stations B and F are relatively closer to the river entrance than the others and therefore demonstrated relatively higher C_{SR}. Figure 20(a) and (b) display the SSS and river discharge time series at Stations B and F to highlight the close inverse correlation between the two properties at the stations.

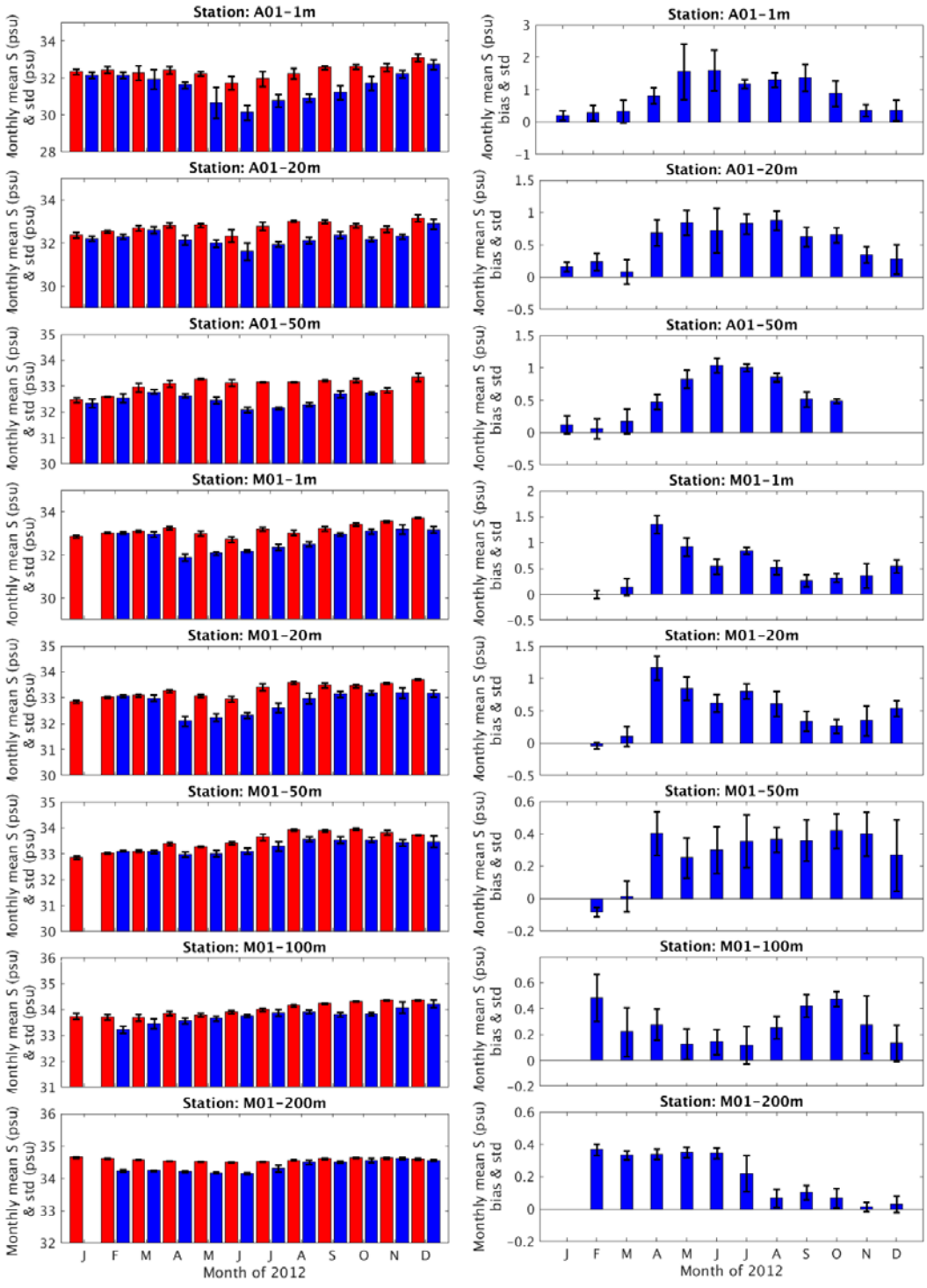

Figure 19. (Left panel) Comparison of the monthly averaged salinity between the model (red bars) and the observations (blue bars) at NERACOOS buoys A01 and M01. The station names and measurement depths are as shown on each plot. On some plots the observations do not appear due to the lack of data. (Right panel) Bias of the monthly mean model temperature. The black lines on top of each bar represent the corresponding standard deviations.

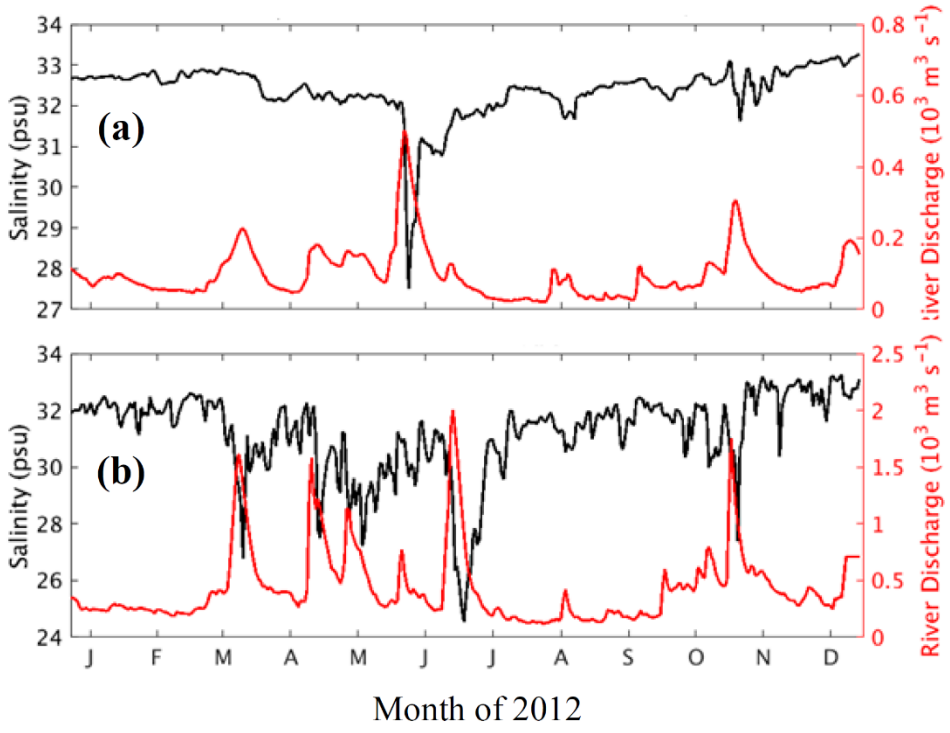

Figure 20. Daily time series of salinity (black lines) and the river discharge Q (red lines) at (a) station B01 (river discharge from the Saco River) and at (b) Station F01 (discharge from the Penobscot River).

6. SUMMARY AND CONCLUSIONS

The NOAA NOS has developed the Gulf of Maine operational nowcast/forecast system (GoMOFS) to produce real-time nowcast and short-range forecast guidance for water levels, 3-dimensional currents, water temperature, and salinity over the broad Gulf of Maine region.

This report describes the GoMOFS system configuration, the hindcast setup, and the verification. GoMOFS was developed using the Regional Ocean Model System (ROMS). The system domain covers the Gulf region including the eastern Long Island Sound, the Gulf of Maine/Georges Bank, and the coast of Nova Scotia (Chapter 2). The grid has horizontal dimensions of 1100 x 770 with approximately 700-m resolution and resolves the water column into 30 layers in the vertical direction. We performed both a tidal forcing only simulation and a one year (2012) period hindcast simulation. The 2012 hindcast simulation included the full suite of forcing factors including tidal and non-tidal water level, current, temperature, and salinity on the open ocean boundary, meteorological forcing on the surface, and river discharge. The tidal forcing data was based on the Oregon State University's TPXO 8.0-Atlas tidal database with some minor adjustment to optimize the model-data agreement (Chapter 3). Other forcing data included the G-RTOFS subtidal water level, current, water temperature, and salinity and the NCEP/NAM's wind stress, heat flux, precipitation, and the USGS river discharge.

We verified the GoMOFS configuration and compared the model outputs with observations (Chapters 4 and 5). Both the tidal only and the hindcast results demonstrate favorable model-data agreement. Over 24 NOS water level stations, the averaged root-mean-squared errors (RMSE) of the tidal amplitude are 4.5, 1.9, 1.4, and 0.6 cm for M_2, S_2, N_2, and K_1, respectively. The corresponding RMSEs for tide phase are 2.8, 5.0, 3.5, and 3.2 degrees.

The hindcast performance was evaluated using the NOS standard skill assessment software and the criteria. The observed data included the time series of water level, T/S, and currents collected by both the NOAA agencies (CO-OPS and NDBC) and the NERACOOS. In general, the hindcast results met the skill assessment criteria (Zhang et al., 2006). The RMSE was about 0.12 m for water level, less than 1.5 °C for temperature, less than 1.5 psu for salinity, less than 0.15 m/s for the current speed, and less than 16 degrees for the current phase. The corresponding central frequency was between 80% and 90% for the water level and generally above 90% for the other properties.

At present, the NOS has implemented the hindcast setup in the NOS standard HPC-COMF environment (Zhang and Yang, 2014), completed a one-year period (March 2016-March 2017) Nowcast/Forecast (N/F) test runs and the associated skill assessment. The model skills fully satisfied the NOS skill assessment criteria. The GoMOFS will be transitioned into operational productions in early FY 2018.

ACKNOWLEDGEMENTS

The authors would like to express sincere gratitude to Drs. John Wilkin, Hernan Arango, Julia Levin, Javier Zavala-Garay at the Rutgers University, to Dr. Ruoying He at the North Carolina State University, and to Dr. Dennis McGillicuddy at Woods Hole Oceanographic Institution for

their valuable comments and detailed technical help on the GoMOFS development. Dr. John Wilkin kindly provided the NAM data (which were pre-processed in the format conforming to the required ROMS requirement) that were used as the hindcast surface forcing. His assistance enabled us to smoothly carry out the GoMOFS development. We would like to express our special thanks for his help. Drs. Lei Shi, John Kelley, and Gregory Seroka in the OCS Coast Survey Development Laboratory kindly reviewed the report. Their valuable comments helped significantly improve the quality of the report. We are sincerely grateful to their help.

REFERENCES

Chen, C., H. Huang, R. C. Beardsley, Q. Xu, R. Limeburner, G. W. Cowles, Y. Sun, J. Qi, and H. Lin (2011), Tidal dynamics in the Gulf of Maine and New England Shelf: An application of FVCOM, *J. Geophys. Res.,* 116, C12010, doi:10.1029/2011JC007054.

Chen, C., R. C. Beardsley, and P. J. S. Franks. 2001. A 3-D prognostic model study of the ecosystem over Georges Bank and adjacent coastal regions. Part I: physical model. *Deep Sea Research.* 48, 419-456.

Egber, G. and L. Erofeeva, 2002: Efficient Inverse Modeling of Barotropic Ocean Tides. *J. Atmos. Oceanic Technol.*, 19, 183204. Tidal database is available for downloading at http://volkov.oce.orst.edu/tides/tpxo8_atlas.html.

Gangopadhyay, A., Robinson, A.R., Haley Jr., P.J., Leslie, W.G., Lozano, C.J., Bisagni, J.J., Yu, Z., 2003. Feature oriented regional modeling and simulations (FORMS) in the Gulf of Maine and Georges Bank. *Continental Shelf Research* 23 (3–4), 317–353.

Greenburg, D. A., 1983: Modeling the mean barotropic circulation in the Bay of Fundy and Gulf of Maine. *J. Phys. Oceanogr.,* 13, 886-904.

Mehra, A., I. Rivin, Z. Garraffo, B. Rajan, 2015. Upgrade of the Operational Global Real Time Ocean Forecast System, 2015. In: Research Activities in Atmospheric and Oceanic modeling, Ed. Astakhova, WMO/World Climate Research Program Report No. 12/2015. http://www.wcrp-climate.org/WGNE/BlueBook/2015.

Moody, J. A., B. Butnam, R.C. Beardsley, W. S. Brown, P. Daifuku, D. A. Mayer, H.O. Mofjeld, B. Petrie, S. Ramp, P. Smith, and W. R. Wright. (1984). Atlas of Tidal elevation and current observations on the Northeast American Continental Shelf and Slope. *U. S., Geological Survey Bulletin*, U.S. Govermanet Printing Office, Washington, DC, 1611, 122pp.

Naimie, C.E., Loder, J.W., Lynch, D.R., 1994. Seasonal variation of the three-dimensional residual circulation on Georges Bank. *J. Geophys. Res*. 99 (C8), 15967}15989. National Geophysical Data Center (NGDC), 2006. https://www.ngdc.noaa.gov/mgg/global/etopo2.html.

NOS, 2017: Updated: Implementation of new Oceanographic Forecast Modeling System for the Gulf of Maine Effective January 3, 2018, NOS Service Change Notice 17-108 Updated (Available at http://www.nws.noaa.gov/os/notification/scn17-108nos_gomofsaaa.htm).

Shchepetkin, A. F., and J. C. McWilliams, 2005: The Regional Ocean Modeling System: A split-explicit, free-surface, topography following coordinates ocean model, Ocean Modelling, 9, 347-404.

Westerink, J. J., R. A. Luettich and J. C. Muccino. (1993). An Advanced Three-Dimensional Circulation Model for Shelves, Coasts, and Estuaries, Report 3: Development of a Tidal Constituent Database for the Western North Atlantic and Gulf of Mexico. *Technical Report DRP-92-6*, U.S. ACE Waterways Experiment Station, Vicksburg, MS.

Wilkin, J., J. Levin, J. Zavala-Garay, H. Arango, E. Hunter, D. Robertson, N. Fleming. (2013). ROMS 4DVar data assimilation: Mid-Atlantic Bight and Gulf of Maine. http: //maracoos.org/sites/macoora/files/downloads/Wilkin-Rutgers-OMG.pptx

Xue, H., F. Chai, and N. R. Perrigrew. (2000). A model study of the seasonal circulation in the Gulf of Maine. *J. Phys. Oceanogr*., 30, 1,111-1,134.

Xue, H. , etc. The GoMOOS nowcast/forecast system (2005). doi:10.1016/j.csr.2005.04.014.

National Geophysical Data Center, 2006. 2-minute Gridded Global Relief Data (ETOPO2) v2. National Geophysical Data Center, NOAA. doi:10.7289/V5J1012Q

Yang, Z., P. Richardson, Y. Chen, J. G.W. Kelley, E. Myers, F. Aikman, M. Peng, and A. Zhang, 2016. Model Development and Hindcast Simulations of NOAA's Gulf of Maine Operational Forecast System. *J. Mar. Sci. Eng*. 4(4), 77; doi:10.3390/jmse4040077.

Yang, Z., E. P. Myers, I. Jeong, and S. A. White, 2013. VDatum for the Gulf of Maine: Tidal Datums, Marine Grids, and Sea Surface Topography. U.S. Department of Commerce, National Oceanic and Atmospheric Administration, Silver Spring, Maryland, *NOAA Technical Memorandum* NOS CS 31, 50 pp.

Yang, Z. and E. Myers, 2008. Barotropic Tidal Energetics and Tidal Datums in the Gulf of Maine and Georges Bank Region. *Estuarine and Coastal Modeling*, American Society of Civil Engineers, M. L. Spaulding (Ed.), *Proceedings of the 10th International Conference*, Newport, RI, November 2007, 74-94.

Zhang, A., K.W. Hess, E. Wei, and E. Myers, 2006. Implementation of Model Skill Assessment Software for Water Level and Current. *NOAA Technical Report* NOS CS 24, Silver Spring, Maryland, 61 pp.

Zhang, A. and Yang, Z. (2014). Coastal Ocean Modeling Framework on NOAA's High Performance Computer (COMF-HPC); *NOAA Technical Report* NOS CO-OPS 039; National Oceanic and Atmospheric Administration: Silver Spring, MD, USA, 2014; p. 70.